이학박사학위논문

A study on the novel regulators of proteasome

새로운 프로테아좀 조절 단백질에 관한 연구

2015년 8월

서울대학교 대학원

생명과학부

이 원 재

A study on the novel regulators of proteasome

새로운 프로테아좀 조절 단백질에 관한 연구

지도교수 정 용 근

이 논문을 이학박사 학위논문으로 제출함
2015년 6월

서울대학교 대학원
생명과학부

이 원 재

이원재의 이학박사 학위논문을 인준함
2015년 6월

위 원 장 _____(인)

부 위 원 장 _____(인)

위 원 _____(인)

위 원 _____(인)

위 원 _____(인)

A study on the novel regulators of proteasome

A dissertation submitted in partial
Fulfillment of the requirement
for the degree of

DOCTOR OF PHILOSOPHY

to the Faculty of
School of Biological sciences
at
Seoul National University
by

WonJae Lee

Date Approved:
June, 2015

_____

_____

_____

_____

_____

ABSTRACT

A study on the novel regulators of proteasome

WonJae Lee
School of Biological Sciences
The Graduate School
Seoul National University

The proteasome is a large protein complex that degrades diverse proteins in ubiquitine-proteasome system (UPS). Numerous substrates which play roles in many signaling to maintain homeostasis are known to be degraded by the complicated degradation processes. In addition, aberrant regulation in UPS and of this complex is associated with various diseases such as cancer, disorder of immune response and neurodegenerative disease. However, it is not known whether and how this elaborate machinery is regulated by diverse cellular signaling. Thus, discovery of novel proteasome regulators is important to understand UPS-associated cellular function and the pathogenesis of various diseases related to proteasome malfunction. To

identify new proteasome modulators regulating the proteasome activity, a cell-based functional screening was established using Degron-GFP and a collection of cDNA library. In this study, I have isolated iRhom1 as a stimulator of proteasome activity from genome-wide functional screening using cDNA expression and an unstable GFP-degron. Expression level of iRhom1 regulated enzymatic activity and assembly of proteasome complexes. iRhom1 expression was induced by endoplasmic reticulum (ER) stressors, leading to the enhancement of proteasome activity, especially in ER-containing microsomes. iRhom1 interacted with PAC1 and PAC2, the 20S proteasome assembly chaperones, affecting their protein stability by dimerization of them. In addition, iRhom1 deficiency in *D. melanogaster* accelerated the rough-eye phenotype of mutant Huntingtin, while transgenic flies expressing either human iRhom1 or *Drosophila* iRhom showed rescue of the rough-eye phenotype.

S5b was previously identified as a proteasome-assembly chaperone in yeast and a negative regulator of 26S proteasome in mammalian. Although regulation of GRK2 is considered as one of cell death mediators in neuronal cells, the regulation of GRK2 expression is not known. Here, I show that GRK2 is regulated by S5b in neuronal cells and mouse model. GRK2 is down-regulated in the cortex and hippocampus of S5b transgenic mice, a

chronic inflammation model and also reduced by S5b expression in HT22 mouse hippocampal cells. Conversely, knockdown of S5b expression increases GRK2 level through increasing the stability of GRK2 protein, independent of its ability to impair proteasome activity. GRK2 and GRK2 K220R, a kinase dead mutant, similarly interacts with S5b in the mouse cortex and HT22 cells through its C-terminal domain, and this domain also decreases GRK2 level. Membrane targeting of GRK2 is affected by S5b expression, as assessed with immunocytochemistry, fractionation, and surface biotinylation assays. In addition, neurotoxic effect of S5b is suppressed by overexpression of GRK2 but not by GRK2 K220R. Thus, S5b may exert its toxic effect through down-regulation of GRK2, a neurotoxic mediator, in neuronal cells, showing an aberrant role of S5b as a negative regulator of GRK2 in neuronal cell death. In addition, *Psmd5*/S5b knockout mouse was successfully generated by the Cas9/CRISPR-mediated *Psmd5*/S5b knockout cassette and show enhanced proteasome activity compared to aged matched littermates. Together, S5b plays a diverse role in the regulation of proteasome activity under pathologic condition and in neuronal cell death through GRK2. In conclusion, I suggest a novel stress signaling pathway responsible for proteasome regulation and critical role of S5b in neuronal cell death independent of its inhibitory function of proteasome.

Keywords: iRhom1, proteasome, regulation, ER stress, PAC1/2, S5b, GRK2

Student Number: 2008-20372

CONTENTS

LIST OF FIGURES

ABBREVIATIONS

ANOVA	Analysis Of Variance
APP	Amyloid precursor protein
CGI-100	transmembrane emp24 protein transport domain containing 5
CHX	Cycloheximide
CP	Core particle
DMEM	Dulbecco's Modified Eagle's Medium
DMSO	Dimethyl sulfoxide
EDTA	Ethylenediaminetetraacetic acid
EGF	Epidermal growth factor
EGFR	Epidermal Growth Factor Receptor
ER	Endoplasmic Reticulum
ERAD	ER-associated Degradation
FBS	Fetal Bovine Serum
G6PT	glucose-6-phosphatase
GAPDH	Glyceraldehyde 3-phosphate dehydrogenase
GFP	Green Fluorescence Protein

GMR	glass multimer reporter
GRK2	G protein-coupled receptor kinase 2
HA	Hemagglutinin
HEK293T	Human Embryonic Kidney 293T
HRD1	HMG-coA Reductase Degradation
IGF	Insulin-like Growth Factor 1
IFN-γ	Interferon gamma
IgG	Immunoglobulin G
IL-6	Interleukin-6
IP	Immunoprecipitation
kDa	Kilodalton
P4HA2	prolyl 4-hydroxylase subunit alpha-2
PA28	Proteasome activator 28
PAAF1	Proteasomal ATPase-associated factor 1
PAC	Proteasome assembly chaperon
PBS	Phosphate Buffered Saline
PMSF	Phenylmethylsulfonyl fluoride
RHBDL	Rhomboid-like family
RIPA	Radio-Immunoprecipitation Assay
RP	Regulatory particle

RT-PCR	Reverse Transcription-Polymerase Chain Reaction
SDS-PAGE	Sodium Dodecyl Sulfate-Poly Acrylamide Gel Electrophoresis
S.E.M	standard error of the mean
shRNA	Short-hairpin RNA
siRNA	Small interfering RNA
TACE	TNF alpha converting enzyme
TBST	Tris Buffered Saline with Tween-20
TG	Thapsigargin
Tris	Tris (hydroxymethyl) aminomethane
UPR	Unfolded protein responses
UPS	Ubiquitin proteasome system

CHAPTER I

iRhom1 regulates proteasome activity via PAC1/2 under ER stress

Abstract

Proteasome is a protein degradation complex that plays a major role in maintaining cellular homeostasis. Despite extensive efforts to identify protein substrates that are degraded through ubiquitination, the regulation of proteasome activity itself under diverse signals is poorly understood. In this study, we have isolated iRhom1 as a stimulator of proteasome activity from genome-wide functional screening using cDNA expression and an unstable GFP-degron. Downregulation of iRhom1 reduced enzymatic activity of proteasome complexes and overexpression of iRhom1 enhanced it. Native-gel and fractionation analyses revealed that knockdown of iRhom1 expression impaired the assembly of the proteasome complexes. The expression of iRhom1 was increased by endoplasmic reticulum (ER) stressors, such as thapsigargin and tunicamycin, leading to the enhancement of proteasome activity, especially in ER-containing microsomes. iRhom1 interacted with the 20S proteasome assembly chaperones PAC1 and PAC2, affecting their protein stability. Moreover, knockdown of iRhom1 expression impaired the dimerization of PAC1 and PAC2 under ER stress. In addition, iRhom1 deficiency in *D. melanogaster* accelerated the rough-eye phenotype of mutant Huntingtin, while transgenic flies expressing either human iRhom1 or *Drosophila* iRhom showed rescue of the rough-eye phenotype. Together, these results identify a novel regulator of proteasome activity, iRhom1, which functions via PAC1/2 under ER stress.

Introduction

The ubiquitin-proteasome system (UPS) is one of the primary clearance machineries that participate in the degradation of regulated, malfunctioned, misfolded, and damaged proteins by marking them with a poly-ubiquitin chain for loading onto the 26S proteasome (Adams, 2003; Ciechanover, 2005). This elaborate clearance occurs in various cellular compartments, including the nucleus, mitochondria, and endoplasmic reticulum (ER) (Christianson and Ye, 2014; Meusser et al., 2005; Wojcik and DeMartino, 2003). For example, the UPS is responsible for degradation of Mfn1 and Mfn2 mitochondrial fusion proteins in the cytosol (Xu et al., 2011) and degrades nuclear FANC2, ATM, and ATR proteins in response to DNA damage signals in the nucleus (Stone and Morris, 2014). In the ER, many secretory and transmembrane proteins are folded during synthesis and checked for the correct folding by this protein quality control system (Hebert and Molinari, 2007). Misfolded proteins are eventually retro-translocated into the cytosol by ER-associated proteins for degradation by the UPS, an ER-associated degradation (ERAD) process (Yoshida and Tanaka, 2010).

Increasing evidence has shown that the activity and assembly of the proteasome are regulated by specific signals. During IFN-γ signaling, for example, the immunoproteasome is assembled by the induction of several

immune-associated subunits, such as βi or PA28 (Groettrup et al., 1995). It also has been reported that the level of the 20S proteasome assembly chaperone POMP is increased by IFN-γ (Heink et al., 2005). TNF-α signaling has been shown to induce S5b/PSMD5, one of the 19S base proteasome assembly chaperones, which inhibits the assembly and activity of the 26S proteasome by recruiting the proteasomal subunit S7 (Shim et al., 2012). Conversely, deletion of S5b/PSMD5 enhances proteasome activity in *D. melanogaster* and rescues the rough-eye phenotype of the tau fly model. In addition, mild inhibition of the proteasome by proteotoxic stress, such as that induced by the proteasome inhibitor MG132, leads to increased level of TCF11, a major transcription factor for proteasome subunits, and increases the number of proteasomes (Steffen et al., 2010). The thymus expresses the unique proteasome subunit β5t and produces a thymus-specific proteasome complex that is critical for CD8+ cell development (Murata et al., 2007). These previous findings suggest that the proteasome is regulated in a signal- and tissue-specific manner with physiologic and pathologic relevance.

The iRhom1 and 2 are counter parts of drosophila iRhom, member of the Rhomboid protease family that is located in the ER and functions to process EGF or TGF-α. In contrast to other Rhomboid protease family members, iRhom lacks protease catalytic activity and acts as a pseudoprotease that inhibits translocation of EGF ligand family members to the Golgi by binding

to them and targeting them to the proteasome. In a *D. melanogaster* model, loss of drosophila iRhom leads to increased sleep periods as a result of the hyperactivation of EGFR signaling (Zettl et al., 2011). In mammal, iRhom1 and 2 also participate promoting the degradation of EGF [16]. Especially, iRhom2 is essential for TACE trafficking and processing to control TNF in hematopoietic cell (Adrain et al., 2012; Freeman, 2009; McIlwain et al., 2012) and iRhom1 plays a role in survival of several epithelial cancers (Yan et al., 2008) and in the suppression of HIF-α degradation in breast cancer cells (Zhou et al., 2014).

To identify novel factors or signals that regulate proteasome activity, I performed a functional screening and found that iRhom1 regulated proteasome activity independently of EGF signaling. In particular, the expression of iRhom1 was increased under ER stress and thus enhanced proteasome activity, possibly via PAC1 and PAC2.

Materials and methods

Cell culture and transfection

HEK293T (human embryonic kidney cell) and SH-SY5Y (human neuroblastoma) cells were obtained from the American Type Culture Collection (ATCC) and cultured in DMEM containing 10% fetal bovine serum and penicillin/streptomycin at 37℃ under 5% CO_2 (v/v). The cells were transfected using LipofectAMINE reagent (Invitrogen) according to the manufacturer's instructions.

Generation of stable cell line

HEK293 and SH-SY5Y cells were transfected either pSuper-Neo or pSuper-Neo-sh-iRhom1 for 24 h and then maintained in selection medium containing 2 mg/ml of G418 (Invitrogen) for 2 weeks. To form stable cell clones, a single cell was further cultivated and the expression level of each cell was analyzed by RT-PCR and western blotting.

Genome-wide functional screening

Functional screening was previously described (Shim et al., 2012). Briefly, for the primary screening, HEK293T cells were culture on a 96-well plate for

24 h and cotransfected with GFP^U and each of 6,200 cDNAs in a mammalian expression vector for 30 h. Then, iRhom1 was isolated among the putative positive cDNA clones reducing GFP^U fluorescence under a fluorescence microscope (Olympus).

Plasmid construction

Plasmid of pCI-FLAG-iRhom1 was kindly provided by Dr. L.Y. Li (University of Pittsburgh, USA) and subcloned into pcDNA-HA. The pcDNA-FLAG-PAC1 and pcDNA-FLAG-PAC2 were kindly provided by Dr. S. Murata (University of Tokyo, Japan) and subcloned into EGFP-N1. HA-RHBDL1, HA-RHBDL2, RHBDL1 S312A, and RHBDL2 S187G were kindly provided by Dr. B. Cohen (Research Corporation Technology, USA). To construct iRhom1, PAC1 and PAC2 shRNA, heteroduplex oligomers containing 5′-UTR or CDS (iRhom1: 5′-AGC TGG ACA TTC CCT CTG C-3′, 5′-TGC CAG GAA CCA TGA GTG A-3′; PAC1: 5′-CCA GAA GCT TGA AGG GTT T- 3′; PAC2: 5′-GCA TAA ATG CTG AAG TGT A-3′) were synthesized, annealed, and cloned into pSuper-Neo (OligoEngine).

Antibodies and western blotting

The following antibodies were used for western blotting and immunoprecipitation assay: anti-iRhom1 (RHBDF1, Sigma-Aldrich), anti-green fluorescent protein (GFP), anti-tubulin, anti-actin, anti-GRP78, anti-Ub

anti-Tom20, anti-Foxred2 and anti-PARP1 (Santa Cruz Biotechnology), anti-S4, anti-S2, anti-β5, anti-S5a, anti-PAC1, anti-PAC2 and anti-20S core (BIOMOL Int). Cells were lyzed by sonication with RIPA buffer (50 mM Tris pH 7.5, 150 mM NaCl, 1% NP-40, 1% sodium deoxycholate, 0.1% SDS) with protease inhibitor cocktail. The lysates were clarified by brief centrifugation, separated by SDS-PAGE, and transferred onto nitrocellulose membranes using a Bio-Rad semi-dry transfer unit (Bio-Rad). Blots were blocked with 5% (w/v) non-fat dry milk in TBS-T solution [25 mM Tris pH 7.5, 150 mM NaCl, and 0.05% (w/v) Tween-20]. Then, the blots were incubated with the indicated antibodies and visualized using the ECL system (GE Healthcare).

Assays for proteasome activities

Cells were rinsed by PBS twice and then lyzed by sonication using rectic buffer (30 mM Tris pH 7.8, 5 mM MgCl2, 10 mM KCl, 0.5 mM DTT, 1 mM ATP) with 1mM of phenylmethylsulphonyl fluoride (PMSF). The lysates were clarified by centrifugation and the activities were measured by use of fluorogenic substrates (Suc-LLVY-AMC, Bz-VGR-AMC, Ac-GPLD-AMC) (BIOMOL) and a fluorometer (EnVision® Multilabel Reader; PerkinElmer) with excitation at 380 nm and emission at 460 nm.

Reverse transcriptase-PCR

Total RNA was prepared using TRI reagent (Molecular Research Center) and cDNA was synthesized by reverse transcriptase (RT; Invitrogen), followed by PCR amplification. PCR was performed for 15-20 cycles using following synthetic oligonucleotides sets: *IRHOM* (5′-ATG GTG GGA CGG CTC ACC-3′, 5′-TTT TGG TGC AGA TCG GCC-3′), *XBP-1* (5′-GAA CCA GGA GTT AAG ACA GC-3′, 5′-AGT CCA TAC CGC CAG AAT CC-3′), *PSMA7* (5′-ATG AGC TAC GAC CGC GCC-3′, 5′-TGA TGC TTT CTT TTG-3′), *PSMG1* (5′-ATG GCG GCC ACG TTC TTC G-3′, 5′-GGT AAC ATG TCG ACA TGT G-3′), *PSMG2* (5′-ATG TTC GTT CCC TGC GGG G-3′, 5′-ATC TAT TTC AGG AAT GCA C-3′), *PSMD5* (5′-AGA TGT TTG GAT GC-3′, 5′-TCA TTC GGC TCC TTC-3′), *PAAF1* (5′-GGG AGT CCT TGC AGA TTG-3′, 5′-TCA GAG GTC AGA AAG CTG-3′), *PSMD9* (5′-ATG TCC GAC GAG GAA GCG-3′, 5′-CAG TGA CTG GAA GTT CTG G-3′) *PSMD4* (5′-AGG AGG AGG CCC GGC-3′, 5′-TCA CTT CTT GTC TTC C-3′), *PSMB10* (5′-ATG CTG AAG CCA GCC CTG-3′, 5′-CTC CAC CTC CAT AGC CTG-3′), *ACTIN* (5′-GAG CTG CCT GAC GGC CAG G-3′, 5′-CAT CTG CTG GAA GGT GGA C-3′).

Subcellular fractionation

Cells were resuspended in buffer (20 mM HEPES pH 7.5, 10 mM KCl, 1.5 mM $MgCl_2$, 1 mM EDTA, 1 mM PMSF), sheared by passing the suspension 30 times through a 26-gauge needle, and then incubated on ice for 20 min in

the presence of 250 mM sucrose. A portion of the samples was saved to check the expression levels of protein between the samples. The cell lysates were centrifuged at 1,000 g for 5 min at 4℃ (nucleus), and the supernatant was further centrifuged at 8,000 g for 20 min at 4℃ (mitochondria). The supernatant was once again centrifuged at 100,000 g for 3 h at 4℃. The resulting pellet contained the microsomal fraction, whereas the supernatant contained cytosol. The pellet of each step was collected, resuspended in buffer, and then used for proteasome activity analysis or native gel analysis.

Glycerol gradient analysis

The 10-40% glycerol gradient analysis was examined as previously described (Tanahashi et al., 2000). Cells were lyzed by sonication in lysis buffer (50 mM Tris pH 7.5, 100 mM NaCl, 0.1 mM EDTA, 2 mM ATP), after which the lysates were centrifuged at 12,000 rpm for 30 min at 4℃. The cell lysates were fractionated by 10-40% (v/v) glycerol density gradient centrifugation (22 h, 100,000 g) and 0.25 ml fractions were collected for analysis.

Immunoprecipitation assay

HEK293T cells were lyzed in a RIPA buffer containing protease inhibitor cocktail. After centrifugation, the supernatant was incubated with FLAG-M2 bead (Sigma Aldrich) at 4℃ for 6 h. For endogenous immunoprecipitation,

HEK293 cells were harvested and then lyzed in a RIPA buffer containing protease inhibitor cocktail. The cells were centrifuged at 12,000 rpm for 20 min at 4℃ and the supernatant was incubated with anti-PAC1 antibody overnight at 4℃ and pulled down by Protein G Sepharose beads (GE Healthcare).

Immunocytochemistry

HeLa cells were cultured on a coverslip coated with poly-L-lysine and then transfected with HA-iRhom1 for 24 h. Cells were fixed with 4% paraformaldehyde and permeabilized with 0.1% Triton X-100. After blocking with 3% FBS in PBS, cells were incubated with anti-HA antibody for 2 h. Samples were observed on a confocal laser scanning microscope (LSM510, Carl Zeiss, Inc.).

Native gel analysis

Native gel analysis was performed as previously described (Elsasser et al., 2005). Cells were lyzed in a rectic buffer and cell lysates were separated by polyacrylamide gel electrophoresis (PAGE) on 4% (w/v) polyacrylamide native-gel at 4℃ (100 V). The gel was overlaid with a buffer containing Suc-LLVY-AMC for 30 min and the fluorescence signal was visualized on a UV trans-illuminator.

Filter trap assay

HEK293T cells cotransfected with HTTex120Q-GFP for 24 h and washed twice with PBS. Cells were then resuspended in PBS containing 1 mM PMSF, sonicated, and then added with PBS containing 1% SDS. Prepared samples were subjected to a filter trap assay using a 96-well dot blot apparatus (Bio-Rad Laboratories). The nitrocellulose membrane was incubated and rinsed with PBS containing 1% SDS, and then analyzed by western blotting using anti-GFP antibody

Drosophila genetics

All crossbreeding experiment and maintenance were carried out at 25℃. Transgenic flies expressing Htt-Q128 (GMR-GAL4/UAS-Htt-Q128) were generously provided by Dr. J.T. Littleton (Massachusetts Institute of Technology, USA). UAS-iRhom and *iRhom* knockout strain were kindly provided by Dr. M. Freeman (University of Oxford, UK). Wild-type (W^{1118}) and IRE1 hetero knockout mutant (CG4583f02170) strains were purchased from the Bloomington Drosophila Stock Center at Indiana University. Transgenic strains expressing human iRhom1 were generated by embryonic injection (Korea Advanced Institute of Science and Technology, Korea).

Results

iRhom1 isolated by functional screening enhances proteasome activity

In a previous study, I employed a functional screening assay utilizing an unstable GFP–degron (GFP^U) system to isolate novel regulators of proteasome activity (Shim et al., 2012). After a gain-of-function screen using 6,200 cDNAs in mammalian expression vectors, I found several clones that greatly reduced the signal of GFP^U upon overexpression. Because iRhom1 was the most effective among them in reducing the GFP signal, I further analyzed the effect of iRhom1 on proteasome activity in detail. Ectopic expression of iRhom1 reduced the GFP^U fluorescence signal by 40% but did not affect the signal of cotransfected RFP (Figure I-1 A). Accordingly, western blot analysis revealed that ectopic expression of iRhom1 reduced the level of GFP^U protein in a concentration- and time-dependent manner (Figure I-2 A and B). When I examined overexpression effects of more than ~100 cDNAs encoding ER membrane proteins, including amyloid precursor protein (APP), prolyl 4-hydroxylase subunit alpha-2(P4HA2), transmembrane emp24 protein transport domain containing 5 (CGI-100), and glucose-6-phosphatase (G6PT), on proteasome activity, I could not observe any significant change in our assay employing GFP^U (Figure I-3 A and B),

indicating that elevation of proteasome activity by iRhom1 is not artificial result of overexpressing a polytopic membrane protein.

Measurement of proteasome catalytic activity using fluorogenic substrates in crude cell extracts revealed that depletion of iRhom1 expression in HEK293T cells significantly decreased the activities of three different enzymes of the proteasome and increased the accumulation of ubiquitin-conjugates (Figure I-4 A and B). Conversely, overexpression of iRhom1 enhanced chymotrypsin-like activity and reduced the amount of ubiquitin conjugates (Figure I-5 A). Similar to the increase of enzyme activities in crude cell extracts, native gel analysis also revealed that overexpression of iRhom1 elevated enzymatic activities of both 30S and 26S proteasomes (Figure I-6 A) and reduced the accumulation of ubiquitin-conjugates induced by the proteasome inhibitor MG132 (Figure I-6 B). These results indicate that iRhom1 regulates proteasome activity. Because iRhom1 is a member of the Rhomboid protease family that regulates the EGF quality control system in the ER (Freeman, 2009), I evaluated whether other members of the Rhomboid family also affect proteasome activity. Overexpression and enzymatic assays revealed that RHBDL1 and RHBDL2 also reduced the level of GFP^{U} and elevated proteasome activity (Figure I-7 A). In addition, the protease activity-dead mutants (RHBDL1 S312A and RHBDL2 S187G) also elevated proteasome activity as much as their wild-type did. These observations

indicate that the Rhomboid protease family affects proteasome activity independently of its reported enzymatic activity.

iRhom1 affects the assembly of proteasome complexes

To address how iRhom1 regulates proteasome activity, I established iRhom1-knockdown stable HEK293 cells using shRNA (Figure I-8 A). Western blot and RT-PCR analysis revealed that iRhom1 deficiency did not affect the levels of the proteasome subunits, including S5a, 20S core, β5 and S2, that were examined (Figure I-8 A and B). Native gel analysis followed by overlay assay using a fluorogenic enzyme substrate revealed that the enzymatic activities of 30S (RP_2CP), 26S (RPCP), and 20S (CP) proteasomes were reduced in iRhom1 knockdown HEK293 cells (Figure I-9 A). The reduced activities of proteasomes were not affected by the addition of SDS (Figure I-9-B). These observations imply that assembly of the proteasomes might be regulated by iRhom1.

To resolve the steps of proteasome assembly in iRhom1-knockdown cells, I performed a fractionation assay using glycerol density gradient centrifugation and analyzed the fractions by western blotting using proteasome subunit-specific antibodies. Compared with control cells, iRhom1-knockdown led to a significant decrease in the levels of S5a, β5, and 20S core in three fraction regions: S5a in the first region comprising fractions

25 – 27 which contained the 30S proteasome, 20S core in the second region including fractions 17 – 19 which contained the 20S proteasome, and β5 in the third region comprising fractions 21 – 23 which contained the 26S proteasome (Figure I-10 A). S5b was shown for control, which was not found in fully assembly proteasome complex (Godderz and Dohmen, 2009). Accordingly, an enzymatic assay revealed that the peptidase activity of the proteasome was also reduced by iRhom1-knockdown in the three fraction regions corresponding to the 20S, 26S, and 30S proteasome complexes, respectively (Figure I-10 B). From similar fractionation assay using gel filtration(Shim et al., 2012), I also observed reduction of 30S proteasome in iRhom1 knockdown cells and increase of assemble intermediates and free subunits (data not shown). Conversely, ectopic expression of iRhom1 did not affect the levels of proteasome subunits but increased the activities of the proteasome complexes as determined by glycerol density gradient fractionation analysis (Figure I-11 A and B, data not shown). These results indicate that iRhom1 regulates the activities of the proteasome complexes through their assembly.

iRhom1 regulates microsomal proteasome activity in response to ER stress

Because the proteasome is found in the nucleus and cytoplasm, and iRhom1 is known to be located in the ER, I evaluated the subcellular location

in which iRhom1 affects proteasome activity. I first confirmed that HA-tagged iRhom1 colocalized with ER-RFP, an ER tracker, but not with Mito-RFP, a mitotracker, or LAPM2-GFP, a lysosome marker (Han et al., 2014), in the transfected HeLa cells (Figure I-12 A). In the subcellular fractionation assay, I detected endogenous iRhom1 in the microsomal fraction containing ER (Figure I-12 B). I then fractionated the cell extracts into the cytosol, nuclear, microsomal, and mitochondrial membrane fractions and compared the proteasome activities of the fractions prepared from wild-type and iRhom1-knockdown cells. Interestingly, catalytic activity of proteasome was reduced to 80% by iRhom1-knockdown only in the microsomal fractions (Figure I-13 A). Conversely, the overexpression of iRhom1 elevated proteasome activity in the microsomal fraction (Figure I-13 B and C). Please note that the level of PAC1, an assembly factor for the 20S proteasome, was significantly reduced in the microsomal fraction of iRhom1-knockdown cells, whereas there was no significant change in the amounts of proteasomal subunits S2 and 20S Core (Figure I-14 A). Consistently, I found that the enzyme activities of the 26S and 30S proteasomes were reduced in the microsomal fraction of iRhom1-knockdown cells as determined by native gel analysis (Figure I-14 B).

I hypothesized that iRhom1 might regulate proteasome activity under ER stress. Therefore, I first examined the expressional regulation of iRhom1 under various ER stresses, such as treatment of cells with thapsigargin,

A23187, and tunicamycin. I found that the level of iRhom1 protein was increased by thapsigargin at 6 h and then returned to the basal level at 12 h in HEK293T cells (Figure I-15 A). Similarly, iRhom1 level was increased by ER stressors in other cells, such as Hep3B human hepatocarcinoma cells and SH-SY5Y neuroblastoma cells (Figure I-16 A). In addition, other inhibitors of protein synthesis, such as geneticin, puromycin, hygromycin, and cycloheximide, potently increased iRhom1 level in those cells. RT-PCR analysis revealed that iRhom1 mRNA level was gradually increased by thapsigargin at 6 h and remained high until 12 h in HEK293T cells (Figure I-15 B) or by geneticin in SH-SY5Y cells (Figure I-16 B). Similarly, proteasome activity was increased by thapsigargin at 6 h and further increased at 12 h (Figure I-15 C).

I then evaluated whether the increase in proteasome activity under ER stress is mediated by iRhom1. In contrast to the thapsigargin-treated control cells, the increase of proteasome activity in the microsomal fraction by ER stress was impaired by down-regulation of iRhom1; the proteasome activity of iRhom1-knockdown cells under ER stress was almost identical to that of untreated control cells (Figure I-17 A). Similarly, native gel analysis revealed that the increase in enzyme activities of the 26S and 30S proteasomes in response to thapsigargin was impaired by iRhom1-knockdown in the microsomal fraction (Figure I-17 B). In addition, the puromycin-mediated increase in proteasome activity of SH-SY5Y cells was also impaired by

iRhom1-knockdown (data not shown). These results suggest that iRhom1 plays an essential role in proteasome activation during ER stress.

iRhom1 increases protein stability and dimerization of PAC1 and PAC2

To gain insight into the role of iRhom1 in the regulation of proteasome assembly, I examined the expression levels of several proteasome assembly chaperones in iRhom1-knockdown cells. As seen in Figure 3d, the level of PAC1 was significantly reduced in iRhom1-knockdown cells. I also found that the level of PAC2 as well as PAC1 was decreased in iRhom1-knockdown HEK293 cells (Figure I-18 A). However, the levels of other assembly chaperones, such as S5b, PAAF1, and p27 proteins, were not related. In contrast to the protein levels, there was no difference in the levels of PAC1 and PAC2 mRNA (Figure I-18 B). When I analyzed the stability of PAC1 protein in the presence of cycloheximide, I found that FLAG-PAC1 protein was stable for 2 h in SH-SY5Y cells. In contrast, FLAG-PAC1 protein was rapidly degraded within 30 min in iRhom1-knockdown SH-SY5Y cells, and this degradation was inhibited by the proteasome inhibitor MG132 (Figure I-19 A). Together, these results suggest that iRhom1 regulates the stability of PAC1 and PAC2 proteins. Consistent with a previous report showing that the interaction between PAC1 and PAC2 increases their protein stability (Hirano et al., 2005), knockdown of PAC1 expression reduced the level of PAC2 protein (Figure I-20 A). Moreover, it appears that downregulation of both

iRhom1 and PAC1 further reduced the level of PAC2 in HEK293T cells. Conversely, overexpression of iRhom1 counteracted the PAC1-dependent reduction of PAC2 level (Figure I-20 B).

Because PAC1 is highly detected together with iRhom1 in the microsomal ER fraction (Figure I-14 A) (Possik et al., 2004) and the initiation of proteasome assembly may occur in the ER(Fricke et al., 2007), I examined the possibility that iRhom1 interacts with PACs. Interestingly, immunoprecipitation analysis revealed that HA-iRhom1 interacted with FLAG-PAC1 and FLAG-PAC2 in the transfected cells (Figure I-21 A) and this interaction was enhanced by iRhom1 overexpression (Figure I-21 B and C). Conversely, knockdown of iRhom1 expression reduced the interaction of endogenous PAC1 and PAC2 (Figure I-22 B). More interestingly, treatment with thapsigargin increased the interaction between PAC1 and PAC2, and this increase was impaired by iRhom1-knockdown (Figure I-22 A and B). I also observed that iRhom1 formed a protein complex with PAC1 and PAC2 in the thapsigargin-treated cells (Figure I-22 A and B). These observations indicate that iRhom1 regulates the interaction between PAC1 and PAC2

iRhom1 relieves mutant Huntingtin aggregation in cells and *Drosophila*

Because it is known that proteasome activity is highly associated with the aggregation of mutant Huntingtin (mtHtt) (Li et al., 2010), I addressed whether iRhom1 contributes to the clearance of mtHtt. Ectopic expression of

HTTex120Q-GFP, a GFP-fused segment of HTT exon 1-containing expanded polyglutamine (n = 120) (Kim et al., 1999), exhibited large and disperse punctate fluorescent patterns in HEK293T cells (Figure I-23 A). Coexpression of HTTex120Q-GFP with iRhom1 remarkably reduced puncta formation of HTTex120Q-GFP in HEK293T cells (Figure I-23 A) and SH-SY5Y cells (Figure I-23 B). As with iRhom1, coexpression with PAC1 or PAC2 also reduced the number of HTTex120Q-GFP aggregates in the same cells. However, overexpression of IRE1 increased the size and number of mtHtt aggregates, as described in our previous study (Lee et al., 2012). Moreover, the filter trap assay showed that ectopic expression of iRhom1, PAC1, or PAC2 reduced the amount of SDS-insoluble aggregates of HTTex120Q-GFP in HEK293T cells (Figure I-23 C). Accordingly, I found that overexpression of PAC1 and/or PAC2 significantly elevated protreasome activity (Figure I-24 A). I previously confirmed that the HTTex120Q-GFP puncta were protein aggregates through immunostaining assays using an anti-ubiquitin antibody and detergent-resistance assays (Noh et al., 2009). These results imply that iRhom1 reduces the accumulation of HTTex120Q-GFP in cultured cells.

To evaluate an *in vivo* role of iRhom1 in the clearance of mtHtt, I established iRhom-knockout (KO1), *Drosophila* iRhom [UAS-iRhom1 (*dr*)]- or human iRhom1 [UAS-iRhom1 (*h*)]-overexpressing flies, and crossed them with Htt-Q128 flies, which express Htt-Q128, display the rough-eye

phenotype, and represent a Huntington disease model (Lee et al., 2004). UAS-iRhom1 (*h*), UAS-iRhom (*dr*), and KO1 flies did not display any detectable alterations in eye phenotype (Figure I-25 A, left upper). Consistent to the assays in cultured cells, overexpression of UAS-iRhom1 (*h*) or UAS-iRhom (*dr*) in Htt-Q128 flies relieved the rough-eye phenotype (Figure I-25 A, left lower). Conversely, knockout of iRhom expression exacerbated the rough-eye phenotype in Htt-Q128 flies (Figure I-25 A). Next, I measured proteasome activity in the head of drosophila. When we first examined developmental defect of drosophila eye in detail, I found that iRhom overexpression itself a little but significantly (5~10%) reduced the numbers of ommatidium in GMR-GAL4 line which expresses iRhom1 (*dr*) and iRhom (*h*) under GAL4 promoter. Then, measurement of the proteasome activity with same numbers of fly heads and normalization by the numbers of ommatidium revealed 5~15% differences of proteasome activity in iRhom-expressing/knockdown neurons compared to control fly (Figure I-26 A and B). Further, measurement of proteasome activity in the heads of iRhom/Htt-Q128 flies and normalization by the numbers of ommatidium also revealed that proteasome activity was significantly decreased by iRhom knockout in Htt-Q128 flies but increased by iRhom overexpression in Htt-Q128 flies (Figure I-25 A, bottom). These results indicate that iRhom1 is effective mediator involved in the clearance of aggregation-prone protein, such as mtHtt.

Figure I-1. Stimulatory effect of iRhom1 overexpression on proteasome activity. (**A**) Accumulation of GFP^U-degron by iRhom1 overexpression. HEK293T cells were cotransfected with GFP^U, RFP, and either pcDNA3 (Ctrl) or iRhom1 for 36 h and then evaluated using a fluorescence microscope (*left*). Relative ratios of GFP^U-positive cells among RFP-positive cells (GFP^U/RFP) were determined (*right*). $*P < 0.05$.

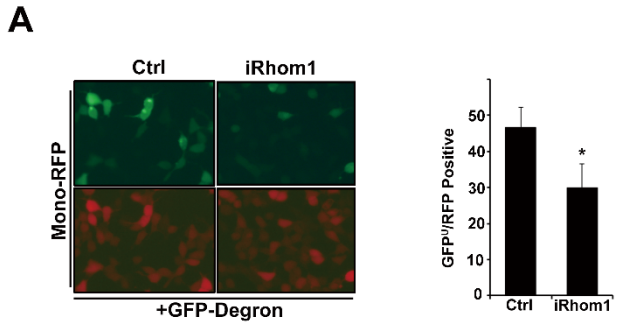
A
Ctrl
iRhom1
Mono-RFP
+GFP-Degron
GFP^U/RFP Positive
50
40
30
20
10
0
*
Ctrl
iRhom1

Figure I-2. Ectopic expression of iRhom1 reduces degron (GFP^U) and elevates proteasome catalytic activity. (**A**) HEK293T cells were cotransfected with GFP^U and the indicated concentrations of FLAG-iRhom1 for 30 h. Cell extracts were prepared and analyzed by western blotting (*top*) or for proteasome activities using Suc-LLVY-AMC (*bottom*). (**B**) HEK293T cells were cotransfected with either pCI-FLAG (Ctrl) or FLAG-iRhom1 for the indicated times. Cell extracts were prepared and analyzed either by western blotting (*left*) or for proteasome activities using Suc-LLVY-AMC (*right*).

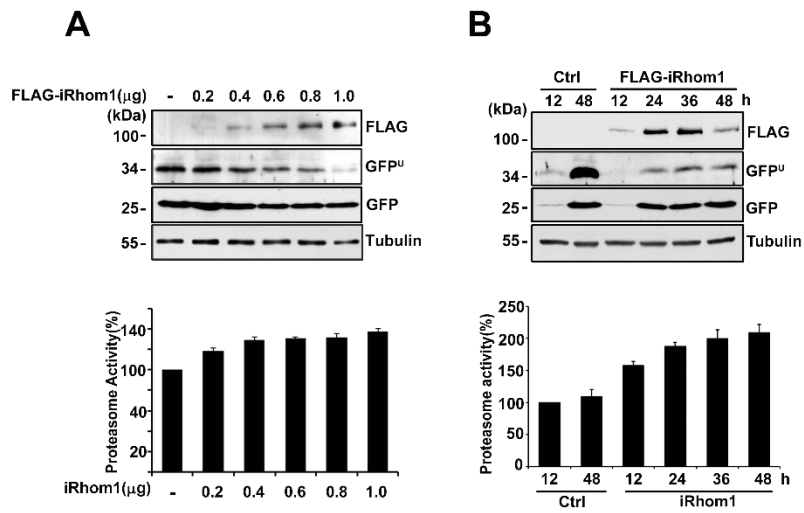
A
FLAG-iRhom1(μg) - 0.2 0.4 0.6 0.8 1.0
(kDa)
100-
34-
25-
55-
FLAG
GFPu
GFP
Tubulin
Proteasome Activity(%)
140
100
40
20
iRhom1(μg) - 0.2 0.4 0.6 0.8 1.0
B
Ctrl
FLAG-iRhom1
12 48 12 24 36 48 h
(kDa)
100-
34-
25-
55-
FLAG
GFPu
GFP
Tubulin
Proteasome activity(%)
250
200
150
100
50
0
12 48 12 24 36 48 h
Ctrl
iRhom1

Figure I-3. Effects of cDNAs encoding polytopic membrane proteins on proteasome activity. (**A**) APP overexpression does not affect GFP^U level and proteasome activity. HEK293T cells were cotransfected with either pcDNA3 (–) or APP (+) with GFP^U for 30 h. Cell extracts were prepared and analyzed either by western blotting (*left*) or for proteasome activities using Suc-LLVY-AMC (*right*). (**B**) Increase of ER membrane proteins does not affect proteasome activity. HEK293T cells were transfected with the indicated cDNAs for 30 h and cell extracts were then analyzed by Suc-LLVY-AMC for proteasome activity.

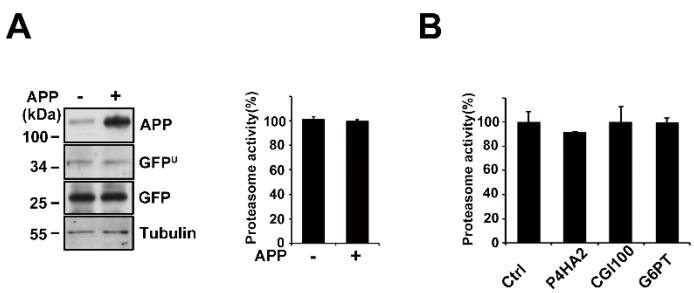
A
APP - +
(kDa)
100
34
25
55
APP
GFPu
GFP
Tubulin
Proteasome activity(%)
100
80
60
40
20
0
APP - +
B
Proteasome activity(%)
100
80
60
40
20
0
Ctrl
P4HA2
CGI100
G6PT

Figure I-4. Downregulation of iRhom1 reduces proteasome activity and increases the accumulation of ubiquitin-conjugates. (**A**) HEK293T cells were transfected with pSuper-Neo (Ctrl) or iRhom1-shRNA (sh-iRhom1) for 48 h and cell extracts were examined for chymotrypsin (Suc-LLVY-AMC), trypsin (Bz-VGR-AMC), and caspase (Ac-GPLD-AMC)-like activities. Bars represent mean values ± S.D. ($n > 3$). *$P < 0.05$. (**B**) iRhom1 modulates the accumulation of ubiquitin-conjugates. After transfection of HEK293T cells with either pSuper-Neo (sh-iRhom1 –) or iRhom1-sh RNA (sh-iRhom1 +) for 48 h, cell extracts were analyzed by western blotting using an anti-ubiquitin antibody.

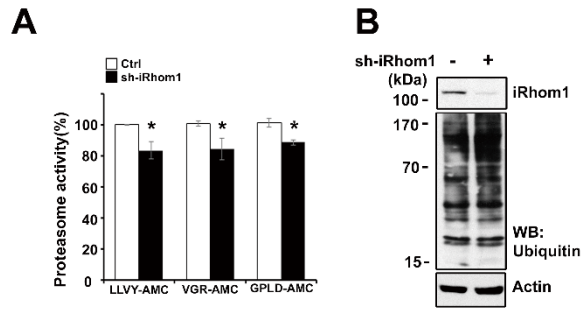
A
Ctrl
sh-iRhom1
Proteasome activity(%)
100
80
60
40
20
0
*
*
*
LLVY-AMC
VGR-AMC
GPLD-AMC
B
sh-iRhom1 - +
(kDa)
100
170
70
15
iRhom1
WB:
Ubiquitin
Actin

Figure I-5. Ectopic expression of iRhom1 increases catalytic activity of proteasome and reduces ub-conjugation. (**A**) After transfection of HEK293T cells with either pcDNA-HA (HA-iRhom1 –) or HA-iRhom1(HA-iRhom1 +) for 30 h, cell extracts were analyzed for chymotrypsin (Suc-LLVY-AMC), trypsin (Bz-VGR-AMC), and caspase (Ac-GPLD-AMC)-like activities (*left*) or analyzed by western blotting using an anti-ubiquitin antibody (*right*). Bars represent mean values ± S.D. ($n > 3$). *$P < 0.05$.

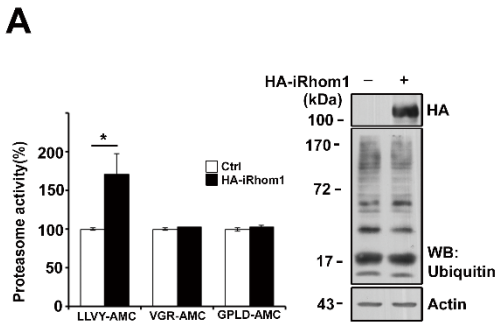
A
HA-iRhom1 – +
(kDa)
100 -
170 -
72 -
17 -
43 -
HA
WB:
Ubiquitin
Actin
Proteasome activity(%)
200
150
100
50
0
*
Ctrl
HA-iRhom1
LLVY-AMC
VGR-AMC
GPLD-AMC

Figure I-6. Ectopic expression of iRhom1 increases proteasome assembly in native gel and reduces MG132 induced ub-conjugation. (**A**) iRhom1 overexpression increases proteasome activity and reduces the accumulation of ubiquitin-conjugates. HEK293T cells were transfected with pcDNA-HA (HA-iRhom1 –) and HA-iRhom1 (HA-iRhom1 +) for 30 h and cell extracts were then separated by Native-PAGE and subjected to overlay assays using Suc-LLVY-AMC (*left*) or western blot (WB) analysis using anti-S5a antibody (*right*). The signal intensities of RP2CP and RPCP in figure (A) were quantified by densitometry and represented with bars for mean values ± S.D. ($n > 3$). $^{**}P < 0.005$ (*right*). (**B**) iRhom1 overexpression reduces the accumulation of ubiquitin-conjugates. HEK293T cells were transfected with pcDNA-HA (Ctrl) and HA-iRhom1 for 24 h and then incubated with or without 1 μM MG132 for 12 h. Cell extracts were then analyzed by western blotting.

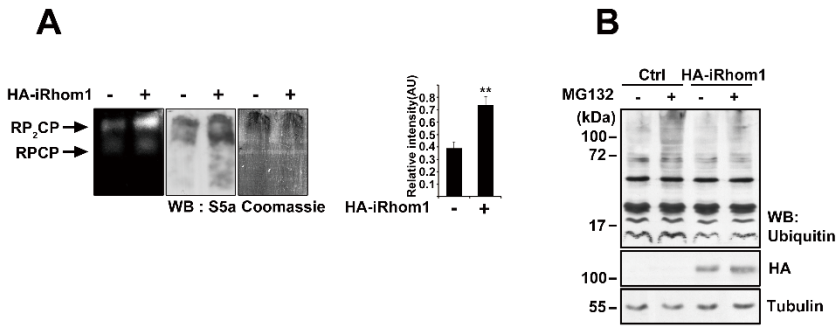
A
HA-iRhom1 - + - + - +
RP2CP
RPCP
WB : S5a Coomassie
Relative intensity(AU)
0.8
0.7
0.6
0.5
0.4
0.3
0.2
0.1
**
HA-iRhom1 - +
B
Ctrl HA-iRhom1
MG132 - + - +
(kDa)
100
72
17
WB:
Ubiquitin
100
HA
55
Tubulin

Figure I-7. Overexpression effects of the Rhomboid protein family and their activity-dead mutants on proteasome activity. (**A**) HEK293T cells were transfected with HA-RHBDL1, HA-RHBDL1 S312A, HA-RHBDL2, or HA-RHBDL2 S187G alone (*lower*), or together with GFP^{U} (*upper*) for 30 h. Cell lysates were analyzed by western blotting using the indicated antibodies (*upper*) or proteasome activity assay using LLVY-AMC (*lower*). Bars represent mean values ± S.D. ($n > 3$).

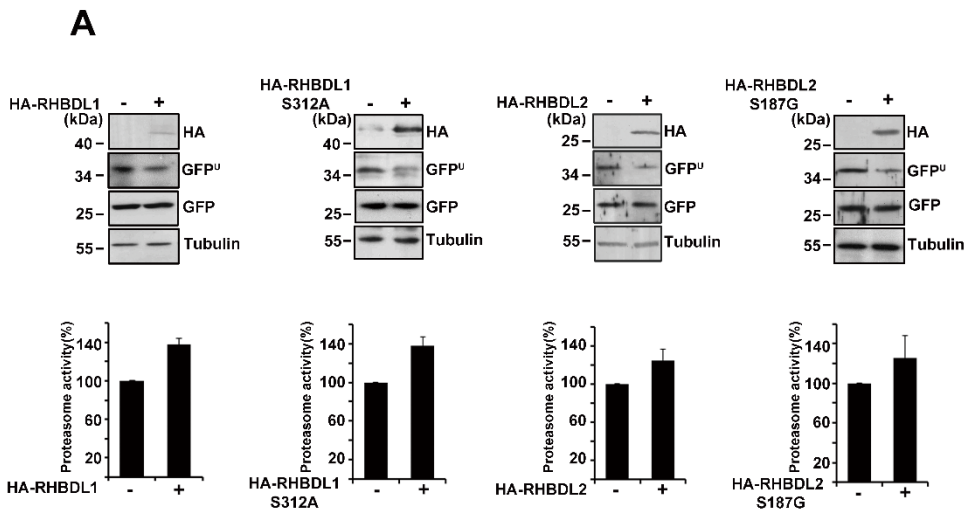
A
HA-RHBDL1
HA-RHBDL1 S312A
HA-RHBDL2
HA-RHBDL2 S187G
(kDa)
HA
GFPU
GFP
Tubulin
Proteasome activity(%)

Figure I-8. iRhom1 does not affect RNA or protein levels of proteasome subunit. (**A**) Expression levels of proteasome subunits in iRhom1-knockdown cells. Cell extracts were prepared from control (Ctrl) and iRhom1-knockdown (sh-Rhom1 #1 and #2) HEK293 cells and analyzed by western blotting using the indicated antibodies. (**B**) Total RNA was purified from HEK293/pSuper-Neo (sh-iRhom1 –) or HEK293/sh-iRhom1 (sh-iRhom1 +) cells and analyzed by RT-PCR

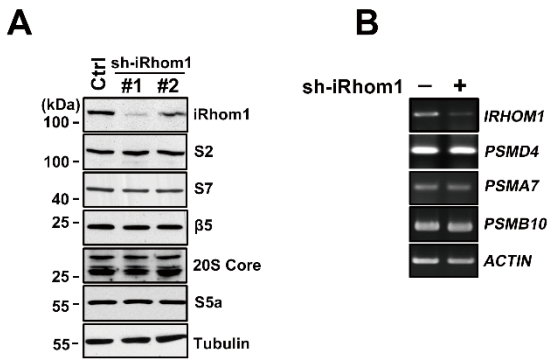
A
Ctrl
sh-iRhom1
#1
#2
(kDa)
100
100
40
25
25
55
55
iRhom1
S2
S7
β5
20S Core
S5a
Tubulin
B
sh-iRhom1 – +
IRHOM1
PSMD4
PSMA7
PSMB10
ACTIN

Figure I-9. **Downregulation of iRhom1 impairs the assembly of proteasome complexes by native gel analysis.** (**A** and **B)** Cell extracts prepared from HEK293/pSuper-Neo (sh-iRhom1 −) or HEK293/iRhom1-shRNA (sh-iRhom1 +) cells were separated by native-PAGE and then analyzed by overlay assays using Suc-LLVY-AMC (A, *left*) or stained with Ponceau S (A, *middle*). RPCP, regulatory particle core particle; CP, core particle. The signals signal intensities of RP2CP and RPCP in figure (A) were quantified by densitometry and represented with bars for mean values ± S.D ($n > 3$) from at least three independent experiments (*right*). $^{**}P < 0.005$. The same cell extracts were examined for proteasome activity in the presence or absence of 0.001% SDS. Bars represent mean values ± S.D. ($n > 3$). (B).

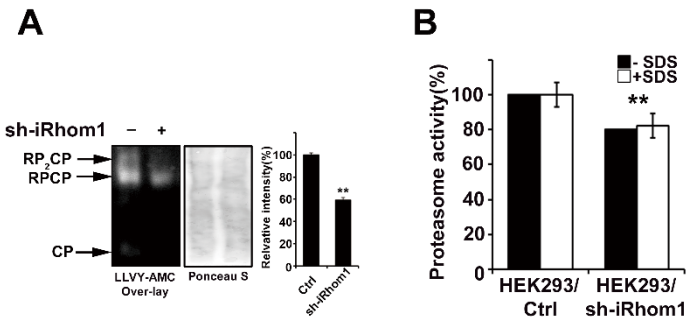
A
sh-iRhom1 – +
RP2CP
RPCP
CP
LLVY-AMC Over-lay
Ponceau S
Relvative intensity(%)
100
80
60
40
20
0
**
Ctrl
shiRhom1
B
- SDS
+SDS
Proteasome activity(%)
100
80
60
40
20
0
**
HEK293/ Ctrl
HEK293/ sh-iRhom1

Figure I-10. Knockdown of iRhom1 expression impairs the assembly of proteasome complexes in a fractionation assay. (**A** and **B**) HEK293T cells were transfected with pSuper-Neo (Ctrl) or iRhom1-shRNA (sh-iRhom1) for 48 h and cell extracts were subjected to sedimentation analysis in a 10–40% (v/v) glycerol gradient. Fractions (250 μl) were collected and analyzed by western blotting after acetone precipitation (A) or proteasome activity assay using Suc-LLVY-AMC (B). The relative positions of 20S, 26S, and 30S proteasome complexes in the fractions are indicated with arrowheads.

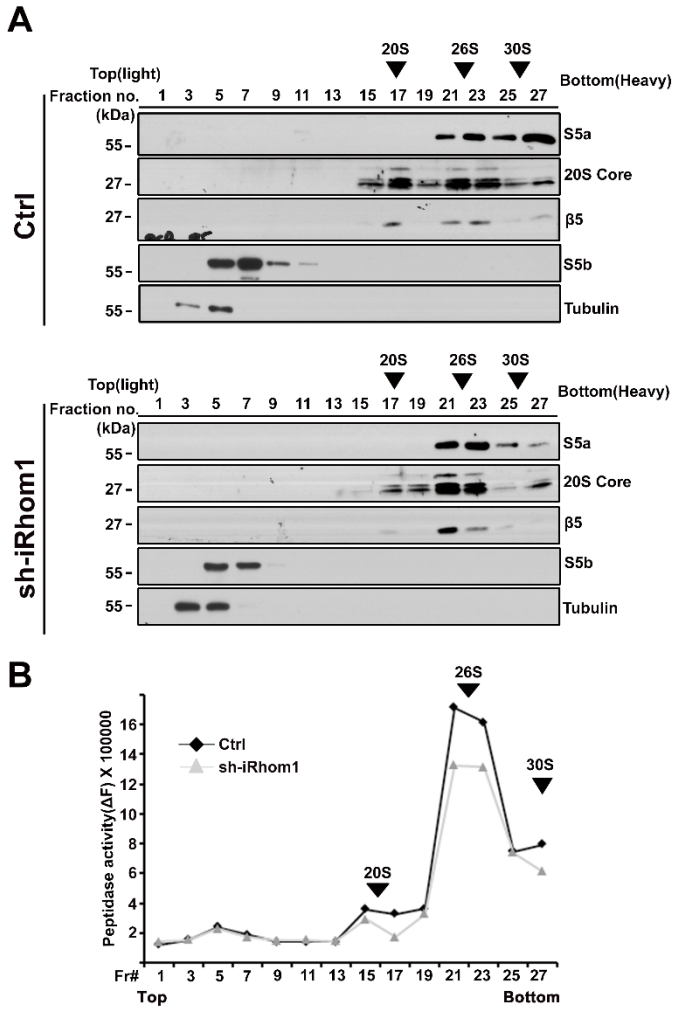
A
Ctrl
sh-iRhom1
Top(light)
Bottom(Heavy)
Fraction no.
(kDa)
20S
26S
30S
S5a
20S Core
β5
S5b
Tubulin
55
27
B
Peptidase activity(ΔF) X 100000
Ctrl
sh-iRhom1
Fr#
Top
Bottom

Figure I-11. Ectopic expression of iRhom1 does not increase protein levels of proteasome subunit but only elevates proteasome activity in fractionation assays. (**A**) HEK293T cells were transfected with either pcDNA-HA (HA-iRhom1 –) or HA-iRhom1 (HA-iRhom1 +) for 30 h and cell extracts were analyzed by western blotting. (**B**) HEK293T cells were transfected with pcDNA-HA (HA-iRhom1 –) or HA-iRhom1 (HA-iRhom1 +) for 30 h and cell extracts were fractionated by glycerol gradient centrifugation and the fractions were assayed for proteasome activity using Suc-LLVY-AMC. Arrowheads indicate the positions of proteasome complexes.

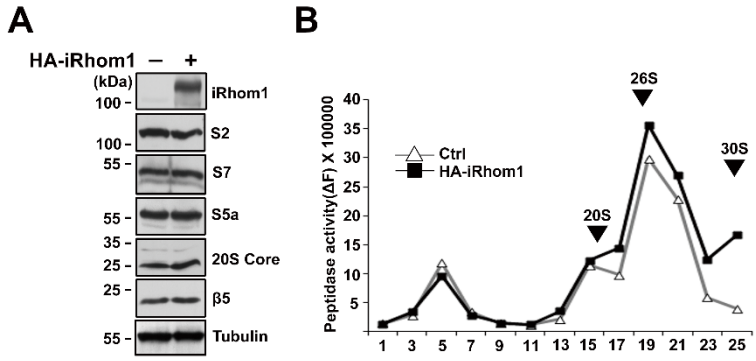
A
HA-iRhom1 – +
(kDa)
100 –
iRhom1
100 –
S2
55 –
S7
55 –
S5a
35 –
25 –
20S Core
25 –
β5
55 –
Tubulin
B
Peptidase activity(ΔF) X 100000
40
35
30
25
20
15
10
5
Ctrl
HA-iRhom1
26S
30S
20S
1 3 5 7 9 11 13 15 17 19 21 23 25

Figure I-12. iRhom1 localizes in the ER of HeLa and HEK293T cells. (**A**) HeLa cells were cotransfected with HA-iRhom1 either EGFP-LAMP2, Mito-RFP or DsRed-Monomer-KDEL for 24 h, stained with anti-HA antibody and Hoechst 33258 (DAPI) for nuclei, and then observed under a confocal microscope. The scale bar represents 20 μm. (**B**) HEK293T cells were fractionated into the nuclear (N), mitochondrial (M), cytosolic (C), and ER-related microsomal (Mi) fractions by ultracentrifugation, and the fractions and total cell lysate (T) were analyzed by western blotting.

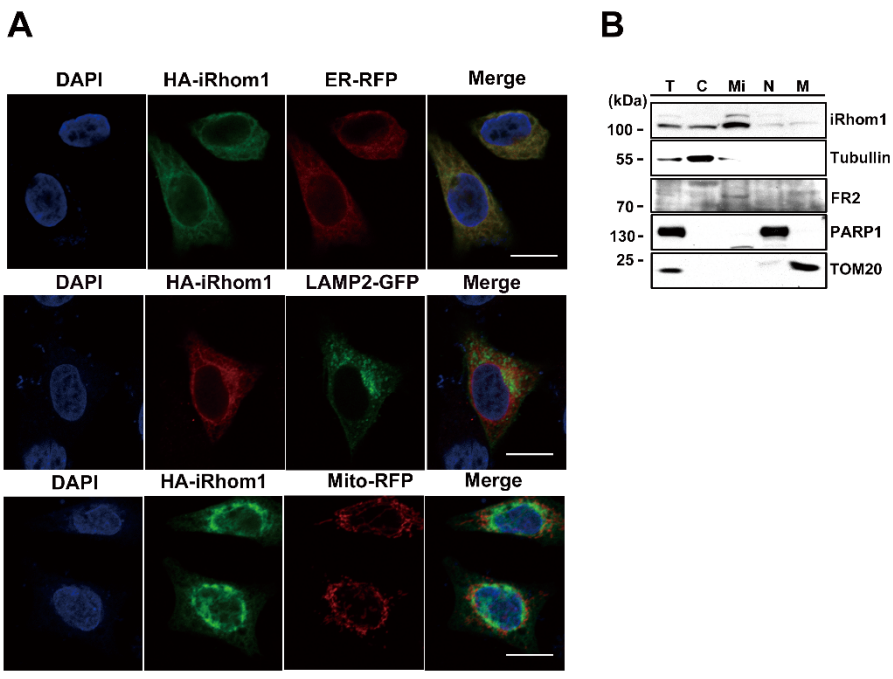
A
DAPI
HA-iRhom1
ER-RFP
Merge
DAPI
HA-iRhom1
LAMP2-GFP
Merge
DAPI
HA-iRhom1
Mito-RFP
Merge
B
T
C
Mi
N
M
(kDa)
100 -
55 -
70 -
130 -
25 -
iRhom1
Tubullin
FR2
PARP1
TOM20

Figure I-13. iRhom1 regulates proteasome activity in the microsomal fractions. (**A**) Cell extracts prepared from HEK293/pSuper-Neo (sh-iRhom1 –) or HEK293/iRhom1-shRNA (sh-iRhom1 +) cells were separated into subcellular fractions as in Figure I-12, and then each fraction was examined for proteasome activity using Suc-LLVY-AMC in the presence or absence of 0.001% SDS. The proteasome activities in total cell extracts and each fraction of control cells were considered 100. Bars represent mean values ± S.D. (n > 3). *P < 0.05. (**B** and **C**) Overexpression of iRhom1 enhances proteasome activity in the microsomal fraction. After transfection of HEK293T cells with pcDNA-HA (HA-iRhom1 –) or HA-iRhom1 (HA-iRhom1 +) for 30 h, cell extracts were fractionated into the cytosol and microsome by ultracentrifugation. Each fraction was then analyzed by western blotting (B) and examined for proteasome catalytic activity using Suc-LLVY-AMC (C). Asterisks indicate non-specific bands. Bars represent mean values ± S.D. (n > 3). *P < 0.05. Short, short exposure; Long, long exposure.

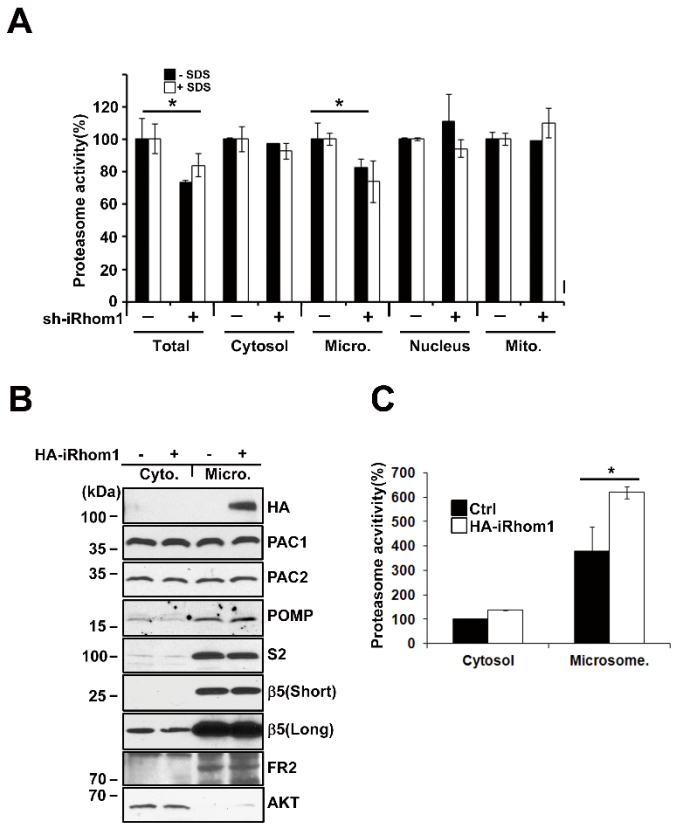
A
- SDS
+ SDS
Proteasome activity(%)
120
100
80
60
40
20
0
*
*
sh-iRhom1
–
+
Total
Cytosol
Micro.
Nucleus
Mito.
B
HA-iRhom1
-
+
Cyto.
Micro.
(kDa)
100 –
HA
35 –
PAC1
35 –
PAC2
15 –
POMP
100 –
S2
25 –
β5(Short)
β5(Long)
70 –
FR2
70 –
AKT
C
Proteasome acvitivity(%)
700
600
500
400
300
200
100
0
Ctrl
HA-iRhom1
*
Cytosol
Microsome.

Figure I-14. iRhom1 regulates proteasome assembly in the microsomal fractions. (**A**) Cell extracts prepared from HEK293/pSuper-Neo (sh-iRhom1 −) or HEK293/iRhom1-shRNA (sh-iRhom1 +) cells were separated into subcellular fractions as in Figure I-12, and then each fraction was analysed by western blotting. Short, short exposure; Long, long exposure. (**B**) Knockdown of iRhom1 expression reduces the assembly and activity of microsomal proteasomes. The cytosolic and ER fractions were separated by native-PAGE and subjected to overlay assays using Suc-LLVY-AMC or western blot (WB) analysis using anti-β5 (WB: β5) and anti-S5a (WB: S5a) antibodies. The signals of S5a in 30S (RP2CP) and 26S (RPCP), and β5 in 20S (CP) on the blot was quantified by densitometry and represented with bars for mean values ± S.D. (n >4). *P < 0.05, **P < 0.005 (*bottom*).

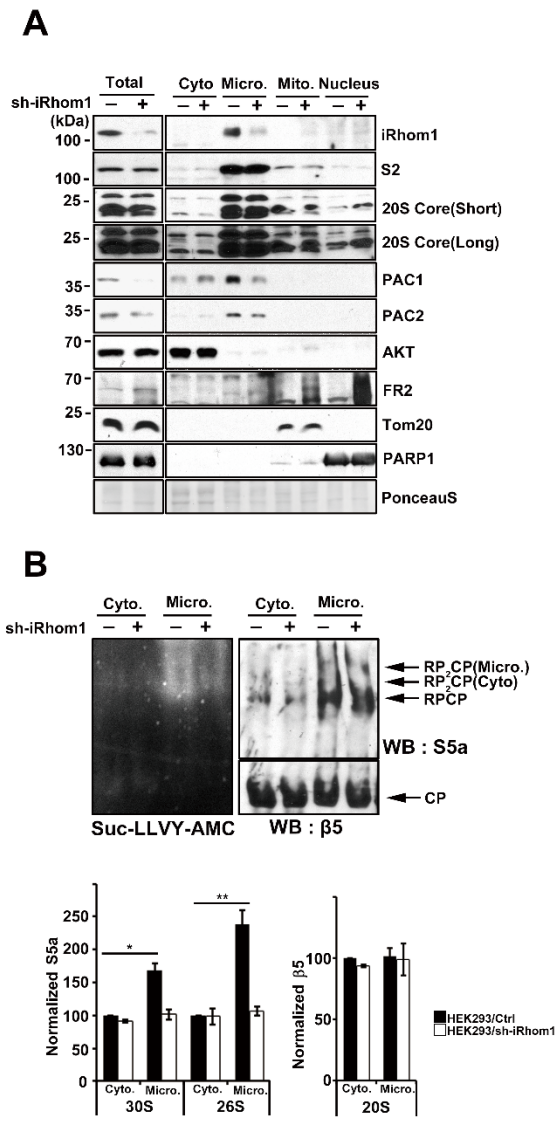
A
Total
Cyto
Micro.
Mito.
Nucleus
sh-iRhom1
(kDa)
100
100
25
25
35
35
70
70
25
130
iRhom1
S2
20S Core(Short)
20S Core(Long)
PAC1
PAC2
AKT
FR2
Tom20
PARP1
PonceauS
B
Cyto.
Micro.
sh-iRhom1
RP2CP(Micro.)
RP2CP(Cyto)
RPCP
WB : S5a
CP
Suc-LLVY-AMC
WB : β5
Normalized S5a
250
200
150
100
50
0
*
**
Cyto.
Micro.
30S
26S
Normalized β5
100
50
0
HEK293/Ctrl
HEK293/sh-iRhom1
20S

Figure I-15. iRhom1 is increased by ER stress (**a**, **b,** and **c**) Thapsigargin treatment increases both iRhom1 expression and proteasome activity. HEK293T cells were treated with 2 μM thapsigargin (TG) for the indicated times and cell extracts were analyzed by western blotting (a) and for proteasome activity using Suc-LLVY-AMC (c). Total RNA was purified from those cells and analyzed by RT-PCR (b). *XBP1u*; unspliced XBP1, *XBP1s*; spliced XBP1. Bars represent mean values ± S.D. ($n > 3$). *$P < 0.05$.

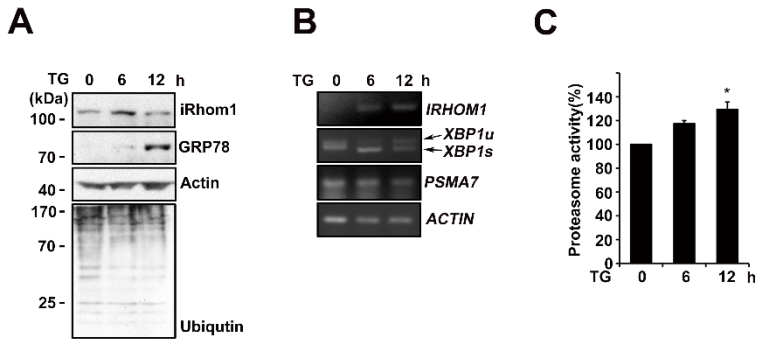
A
TG 0 6 12 h
(kDa)
100
70
40
170
70
25
iRhom1
GRP78
Actin
Ubiqutin
B
TG 0 6 12 h
IRHOM1
XBP1u
XBP1s
PSMA7
ACTIN
C
Proteasome activity(%)
140
120
100
80
60
40
20
0
TG 0 6 12 h
*

Figure I-16. Increase in iRhom1 expression by stress signals. (**A** and B) Increase in iRhom1 by ER stressors and translation inhibitors. Hep3B cells and SH-SY5Y cells were left untreated (Mock) or incubated with geneticin (1 mg/ml) for 24 h (*left*) and 12 h (*right two*), tunicamycin (Tuni., 2 μM) for 24 h (*left*) and 12 h (*right two*), thapsigargin (TG, 1 μM), A23187 (1 μM), cycloheximide (CHX., 1 μg/ml), puromycin (Puro., 150 μM), hygromycin (Hygro., 150 μg/ml) and chloramphenicol (Chlora., 150 μg/ml) for 12 h (*right two*). Cell extracts were analyzed by western blotting (A) and total RNA isolated from SH-SY5Y cells was analyzed by RT-PCR (B).

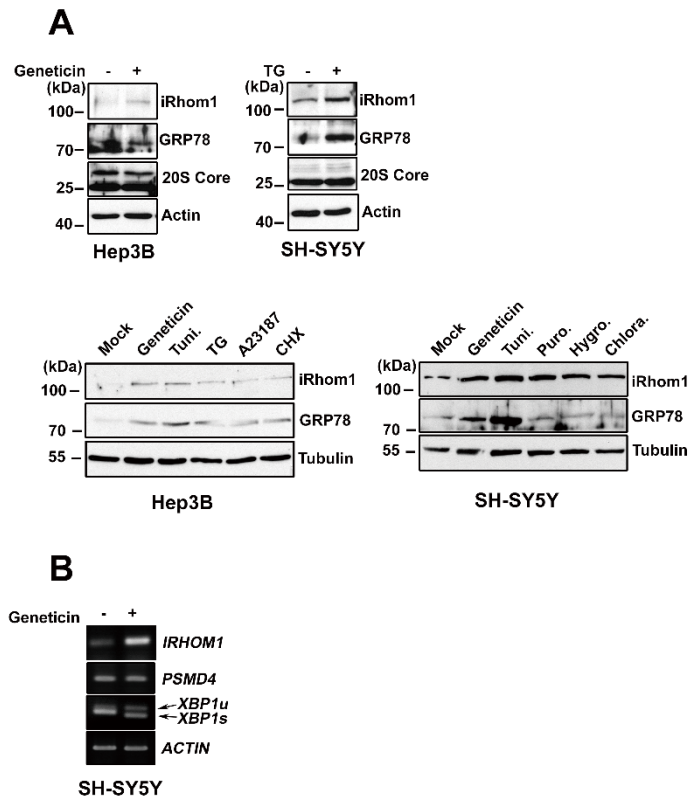
A
Geneticin - +
(kDa)
100
70
25
40
iRhom1
GRP78
20S Core
Actin
Hep3B
TG - +
(kDa)
100
70
25
40
iRhom1
GRP78
20S Core
Actin
SH-SY5Y
Mock
Geneticin
Tuni.
TG
A23187
CHX
(kDa)
100
70
55
iRhom1
GRP78
Tubulin
Hep3B
Mock
Geneticin
Tuni.
Puro.
Hygro.
Chlora.
(kDa)
100
70
55
iRhom1
GRP78
Tubulin
SH-SY5Y
B
Geneticin - +
IRHOM1
PSMD4
XBP1u
XBP1s
ACTIN
SH-SY5Y

Figure I-17. Knockdown of iRhom1 expression impairs ER stress-induced activation and assembly of proteasomes in the microsomal fraction. (**A**) After treatment with 2 μM thapsigargin (TG) for 6 h, cell extracts were prepared from HEK293/pSuper-Neo (sh-iRhom1 –) or HEK293/iRhom1-shRNA (sh-iRhom1 +) cells and fractionated into the nuclear, mitochondrial, cytosolic, and ER-containing microsomal fractions by ultracentrifugation and each fraction was examined for proteasome activity using Suc-LLVY-AMC in the presence or absence of 0.001% SDS. Bars represent mean values ± S.D. (n > 3). (**B**) Knockdown of iRhom1 expression impairs ER stress-induced proteasome assembly in the microsomal fraction. After treatment with 2 μM thapsigargin (TG) for 6h, cell extracts prepared from HEK293/pSuper-Neo (sh-iRhom1 –) or HEK293/iRhom1-shRNA (sh-iRhom1 +) cells were fractionated by ultracentrifuge. Collections of ER fraction were resolved by native-PAGE and then analyzed by overlay assays using Suc-LLVY-AMC (*left*). The blot was stained with Ponceau S (*middle*). The signal intensities of RP2CP and RPCP in figure (c) were quantified by densitometry and represented with bars for mean values ± S.D. (n = 5). *P < 0.05, **P < 0.005 (*right*).

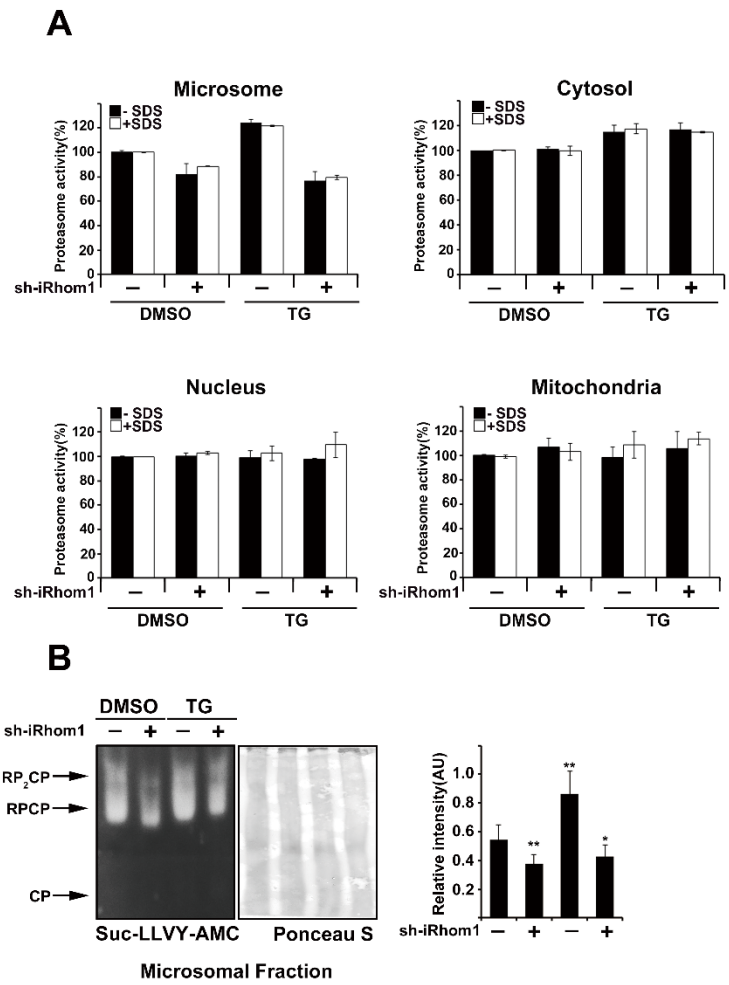
A
Microsome
Cytosol
Nucleus
Mitochondria
- SDS
+SDS
Proteasome activity(%)
sh-iRhom1
DMSO
TG
B
RP2CP
RPCP
CP
Suc-LLVY-AMC
Ponceau S
Microsomal Fraction
Relative intensity(AU)

Figure I-18. The amounts of PAC1 and PAC2 proteins are decreased by iRhom1-knockdown. (**A**) Cell extracts prepared from HEK293/pSuper-Neo (Ctrl) or HEK293/iRhom1-shRNA (#1 and #2) cells were analyzed by western blotting. (**B**) iRhom1 does not affect RNA levels of proteasome assembly chaperones. Total RNA was isolated and analyzed by RT-PCR.

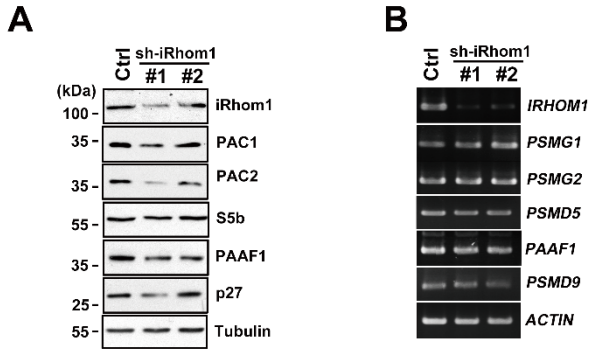
A
Ctrl
sh-iRhom1
#1
#2
(kDa)
100
35
35
55
35
25
55
iRhom1
PAC1
PAC2
S5b
PAAF1
p27
Tubulin
B
Ctrl
sh-iRhom1
#1
#2
IRHOM1
PSMG1
PSMG2
PSMD5
PAAF1
PSMD9
ACTIN

Figure I-19. iRhom1 enhances the stability of PAC1 protein. (**A**) Downregulation of iRhom1 reduces the stability of exogenous FLAG-PAC1. SH-SY5Y/pSuper-Neo (Ctrl) or SH-SY5Y/sh-iRhom1 (sh-iRhom1) cells were cotransfected with FLAG-PAC1 and EGFP for 30 h and then incubated with 100 μg/ml cycloheximide (CHX) and/or 10 μM MG132 for the indicated times. Cell lysates were prepared and analyzed by western blotting (*left*). The signals of FLAG-PAC1 on the blots were quantified using ImageJ software (r*ight*). (**B**) HeLa cells were treated with 200 μg/ml cycloheximide (CHX) with/without MG132 for the indicated times and analyzed with western blotting (*left*). The signals of PAC1 on the blots were quantified using ImageJ software (*right*). (**C**) HEK293/pSuper-Neo (HEK293/Ctrl) or HEK293/sh-iRhom1 cells were incubated with 200 μg/ml cycloheximide (CHX) for the indicated times. Cell lysates were prepared and analyzed by western blotting (*left*). The signals of PAC1 on the blots were quantified using ImageJ software (*right*). (**c**) Total cell lysates of the indicated cell lines were analyzed by western blotting.

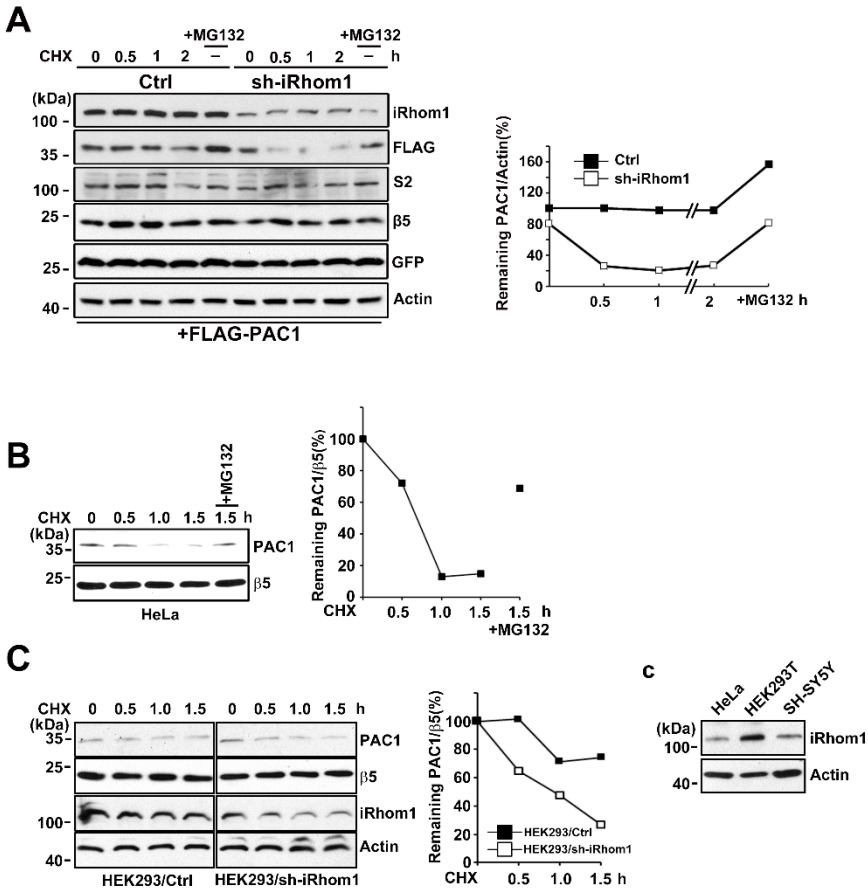
A
+MG132
+MG132
CHX 0 0.5 1 2 – 0 0.5 1 2 – h
Ctrl
sh-iRhom1
(kDa)
100 -
35 -
100 -
25 -
25 -
40 -
iRhom1
FLAG
S2
β5
GFP
Actin
+FLAG-PAC1
Remaining PAC1/Actin(%)
160
120
80
40
0
Ctrl
sh-iRhom1
0.5
1
2
+MG132 h
B
+MG132
CHX 0 0.5 1.0 1.5 1.5 h
(kDa)
35-
25-
PAC1
β5
HeLa
Remaining PAC1/β5(%)
100
80
60
40
20
0
CHX 0.5 1.0 1.5 1.5 h
+MG132
C
CHX 0 0.5 1.0 1.5 0 0.5 1.0 1.5 h
(kDa)
35-
25-
100-
40-
PAC1
β5
iRhom1
Actin
HEK293/Ctrl
HEK293/sh-iRhom1
Remaining PAC1/β5(%)
100
80
60
40
20
0
HEK293/Ctrl
HEK293/sh-iRhom1
CHX 0.5 1.0 1.5 h
c
HeLa
HEK293T
SH-SY5Y
(kDa)
100-
40-
iRhom1
Actin

Figure I-20. iRhom1 regulates the stability of PAC1 and PAC2 proteins. (**A**) Knockdown of PAC1 expression reduces the amount of PAC2 protein. HEK293/pSuper-Neo(sh-iRhom1 –) and HEK293/iRhom1-shRNA (sh-iRhom1 +) cells were transfected with pSuper-Neo (Ctrl), PAC1-shRNA (sh-PAC1), and/or iRhom1-shRNA for 72 h, as indicated, and cell lysates were analyzed by western blotting. (**B**) Stability of PAC1 and PAC2 proteins are increased by iRhom1 overexpression. HEK293T cells were transfected with HA-iRhom1 and pSuper-Neo (Ctrl) or pSuper-Neo-PAC1 (sh-PAC1) for 70 h. Cell lysates were prepared and analyzed by western blotting.

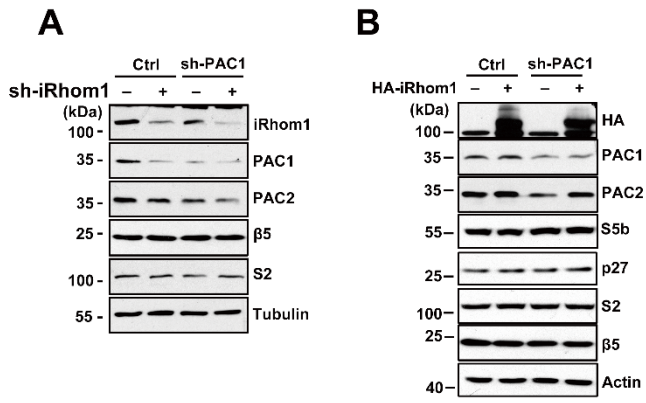
A
Ctrl
sh-PAC1
sh-iRhom1
– + – +
(kDa)
100 -
35 -
35 -
25 -
100 -
55 -
iRhom1
PAC1
PAC2
β5
S2
Tubulin
B
Ctrl
sh-PAC1
HA-iRhom1
– + – +
(kDa)
100 –
35 –
35 –
55 –
25 –
100 –
25 –
40 –
HA
PAC1
PAC2
S5b
p27
S2
β5
Actin

Figure I-21. iRhom1 affects the interaction between PAC1 and PAC2. (**A**) HEK293T cells were cotransfected with FLAG-PAC1, FLAG-PAC2, and HA-iRhom1 for 30 h. Cell lysates were analyzed by immunoprecipitation (IP) assay with anti-FLAG-M2 beads or anti-PAC1 antibody, followed by western blotting using the indicated antibodies. HC indicate the heavy chains of immunoglobulin. (**B** and **C**) iRhom1 affects the interaction of PAC1 and PAC2. HEK293T cells were cotransfected with GFP-PAC1, FLAG-PAC2, and HA-iRhom1 (B) or HA-iRhom1 only (C) for 30 h. Cell lysates were analyzed by immunoprecipitation (IP) assay with anti-FLAG-M2 beads, followed by western blotting using the indicated antibodies. LC indicates the light chains of immunoglobulin.

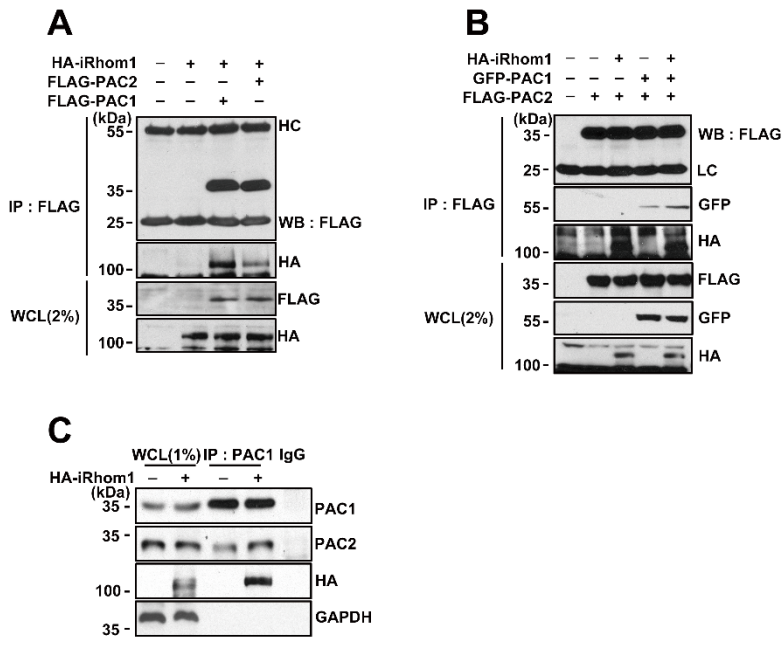
A
HA-iRhom1 – + + +
FLAG-PAC2 – – – +
FLAG-PAC1 – – + –
(kDa)
55-
35-
25-
100-
IP : FLAG
WCL(2%)
HC
WB : FLAG
HA
35-
FLAG
100-
HA
B
HA-iRhom1 – – + – +
GFP-PAC1 – – – + +
FLAG-PAC2 – + + + +
(kDa)
35-
25-
55-
100-
IP : FLAG
WCL(2%)
WB : FLAG
LC
GFP
HA
35-
FLAG
55-
GFP
100-
HA
C
WCL(1%)
IP : PAC1 IgG
HA-iRhom1 – + – +
(kDa)
35 -
35 -
100 -
35 -
PAC1
PAC2
HA
GAPDH

Figure I-22. ER stress increases PAC1/PAC2 dimerization in an iRhom1-dependent manner. (**A**) Thapsigargin treatment increases PAC1 and PAC2 dimerization. HEK293T cells were treated with 2 μM thapsigargin (TG) for 6 h and cell extracts were analyzed by immunoprecipitation (IP) assay using an anti-PAC1 antibody. Whole cell lysates (WCL, 2% of input) and the immunoprecipitates were analyzed by western blotting. (**B**) HEK293/pSuper-Neo (sh-iRhom1 −) or HEK293/sh-iRhom1 (sh-iRhom1 +) cells were left untreated (Mock) or incubated with 2 μM thapsigargin (TG) for 6 h. Then, cell extracts were prepared and subjected to immunoprecipitation (IP) assay using an anti-PAC1 antibody. Whole cell lysates (WCL) and the immunoprecipitates were analyzed by western blotting.

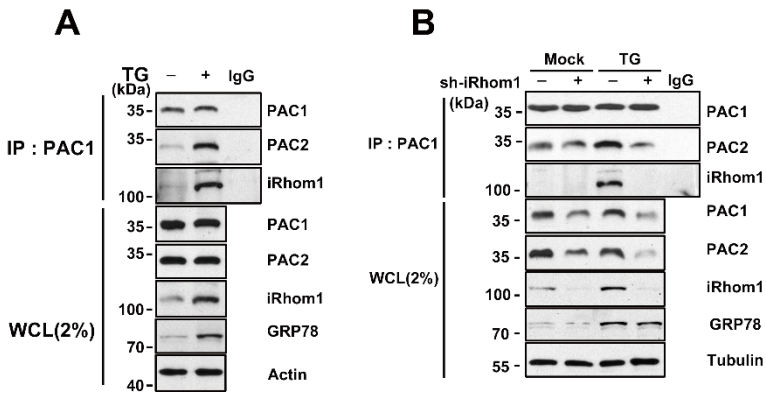
A
TG
(kDa)
–
+
IgG
IP : PAC1
35
35
100
PAC1
PAC2
iRhom1
WCL(2%)
35
35
100
70
40
PAC1
PAC2
iRhom1
GRP78
Actin
B
Mock
TG
sh-iRhom1
–
+
–
+
IgG
(kDa)
IP : PAC1
35
35
100
PAC1
PAC2
iRhom1
WCL(2%)
35
35
100
70
55
PAC1
PAC2
iRhom1
GRP78
Tubulin

Figure I-23. Expression level of iRhom1 modulates the aggregation of mutant Huntingtin in cells. (**A**, **B,** and **C**) Ectopic expression of iRhom1 reduces the aggregation of mutant huntingtin (mtHTT) in HEK293T cells and SH-SY5Y neuroblastoma cells. HEK293T cells (A) and SH-SY5Y cells (B) were co-transfected with pHTTex120Q-GFP (mtHTT), RFP, and pcDNA (Ctrl), iRhom1, PAC1, PAC2, or IRE1. After 30 h, cells were examined for the aggregation (arrows) of mtHTT by fluorescence microscopy (a) and for the percentages of cells showing mtHTT aggregates among total GFP-positive cells (B). Transfection efficiency was normalized by RFP. Bars represent mean values ± S.D. (n = 3). HEK293T cell extracts were then prepared and subjected to a filter trap assay as described in Materials and Methods (C).

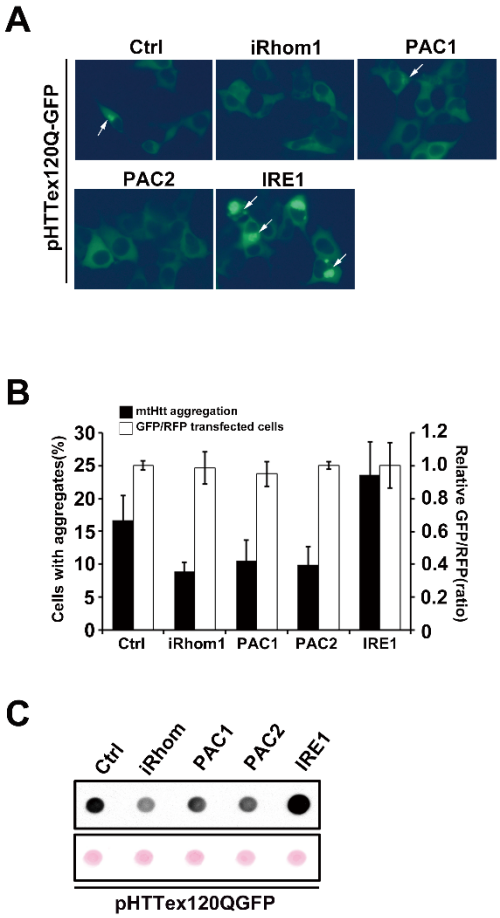
A
Ctrl
iRhom1
PAC1
pHTTex120Q-GFP
PAC2
IRE1
B
mtHtt aggregation
GFP/RFP transfected cells
Cells with aggregates(%)
Relative GFP/RFP(ratio)
30
25
20
15
10
5
0
1.2
1.0
0.8
0.6
0.4
0.2
0
Ctrl
iRhom1
PAC1
PAC2
IRE1
C
Ctrl
iRhom
PAC1
PAC2
IRE1
pHTTex120QGFP

Figure I-24. Ectopic expression of PAC1 and PAC2 elevates proteasome activity. (**A**) HEK293T cells were transfected with PAC1, PAC2, or both PAC1 and PAC2 for 30 h. Cell extracts were prepared and analyzed for proteasome activity using Suc-LLVY-AMC (*left*) or western blotting (*right*).

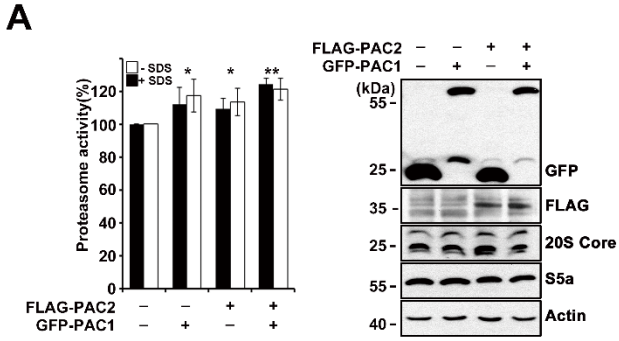
A
- SDS
+ SDS
Proteasome activity(%)
120
100
80
60
40
20
0
*
*
**
FLAG-PAC2 – – + +
GFP-PAC1 – + – +
FLAG-PAC2 – – + +
GFP-PAC1 – + – +
(kDa)
55
25
35
25
55
40
GFP
FLAG
20S Core
S5a
Actin

Figure I-25. Expression level of iRhom1 modulates the aggregation of the rough-eye phenotype in a fly model expressing Htt120Q. (**A**) iRhom is critical for the regulation of rough-eye phenotype and proteasome activity in a fly model expressing mutant huntingtin (Htt128Q). Wild-type (w^{1118}), iRhom-knockout (KO1), iRhom (*Drosophila* form)-overexpressing [UAS-iRhom (*dr*)] or iRhom1 (human form)-overexpressing [UAS-iRhom1 (*h*)] flies were crossed with flies expressing Htt128Q. (*left*) The presence or absence of the rough-eye phenotype was then evaluated using a stereo microscope and the numbers of ommatidium of each drosophila eye were counted. Proteasome activity in the same numbers of fly heads in each group was measured and normalized by the numbers of ommatidium. Data are means ± SEM (***$P < 0.005$, $n = 15$).

A

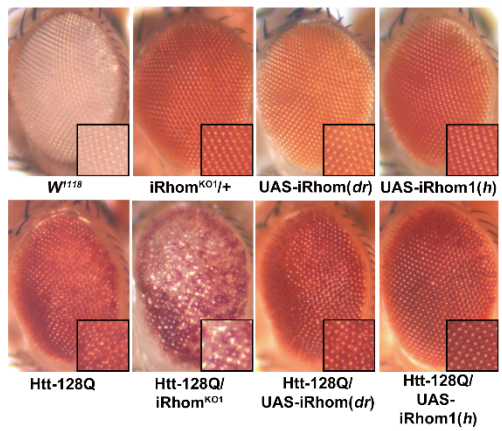
W1118
iRhomKO1/+
UAS-iRhom(dr)
UAS-iRhom1(h)
Htt-128Q
Htt-128Q/ iRhomKO1
Htt-128Q/ UAS-iRhom(dr)
Htt-128Q/ UAS-iRhom1(h)

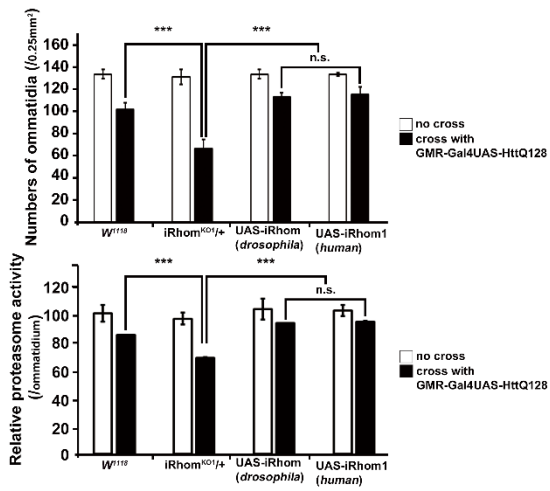
Numbers of ommatidia (/0.25mm²)
***
***
n.s.
no cross
cross with GMR-Gal4UAS-HttQ128
W1118
iRhomKO1/+
UAS-iRhom (drosophila)
UAS-iRhom1 (human)
Relative proteasome activity (/ommatidium)

Figure I-26. Overexpression of drosophila iRhom or human iRhom1 in drosophila eye shows mild disturbance in eye development and increases proteasome activity. (**A**) Single overexpression of drosophila or human form of iRhom leads to decrease in the numbers of ommatidium in drosophila eye. Wild-type (w^{1118}), iRhom-knockout (KO1), iRhom (*Drosophila* form)-overexpressing [UAS-iRhom (*dr*)] or iRhom1 (human form)-overexpressing [UAS-iRhom1 (*h*)]. (**B**) Overexpression of drosophila or human form of iRhom increases proteasome activity in the ommatidium of flies. Proteasome activity was measured in the fly head extracts and normalized by the numbers of ommatidium in each group. Data are the means ± SEM (***$P < 0.005$, *$P < 0.05$, $n = 15$).

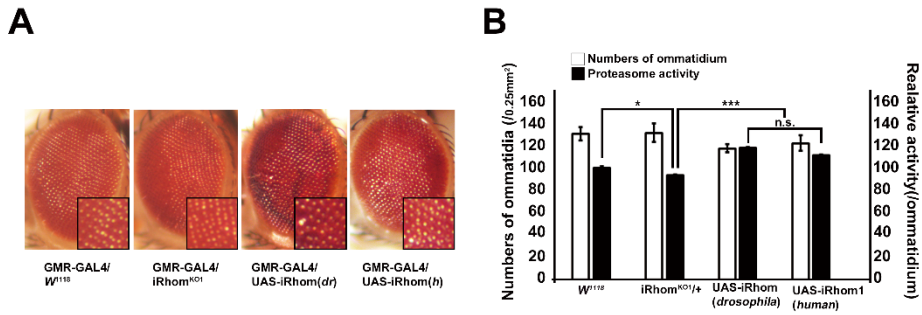
A
B
GMR-GAL4/ W1118
GMR-GAL4/ iRhomKO1
GMR-GAL4/ UAS-iRhom(dr)
GMR-GAL4/ UAS-iRhom(h)
Numbers of ommatidium
Proteasome activity
Numbers of ommatidia (/0.25mm2)
Realative activity(/ommatidium)
0
20
40
60
80
100
120
140
160
*
***
n.s.
W1118
iRhomKO1/+
UAS-iRhom (drosophila)
UAS-iRhom1 (human)

Figure I-27. Schematic diagram showing the proposed role of iRhom1 in proteasome activation under ER stress. ER-stress increases iRhom1, which results in enhanced dimerization of PAC1 and PAC2 and elevates proteasome activity.

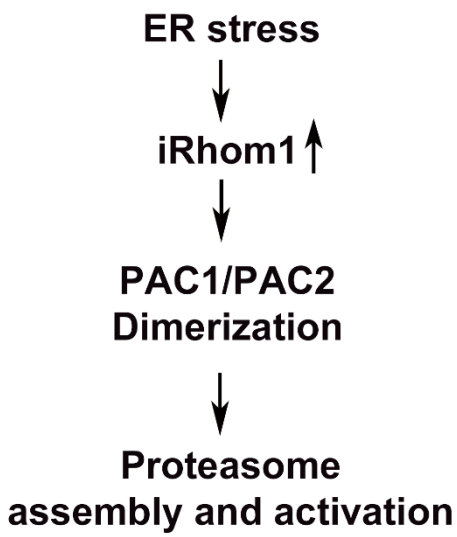
ER stress
iRhom1
PAC1/PAC2
Dimerization
Proteasome
assembly and activation

Discussion

Compared with other rhomboid-like family members, iRhom1 does not have a catalytic serine residue and inhibits the secretion of EGF, a rhomboid substrate, which is essential for cell survival (Yan et al., 2008). While some growth factors, such as IGF-I, increase proteasome activity (Crowe et al., 2009), the proposed role of iRhom1 in the processing of EGF is inhibitory in growth factor secretion (Zettl et al., 2011). In addition, when I treated HEK293 cells with EGF, there was no significant difference in proteasome activity between wild-type cells and iRhom1-knockdown cells (data not shown). These observations all indicate that the stimulatory activity of iRhom1 on proteasome is not associated with the protease activity of the rhomboid-like family of proteins and is independent of EGF activity. Recently, several reports showed that rhomboid family Derlin-1 and RHBDL4 also facilitates ERAD and interacts with p97/VCP for substrate degradation independently of protease activity (Fleig et al., 2012; Greenblatt et al., 2011). Perhaps, this interaction between rhomboid family and common factor p97/VCP may explain our observation that why all of rhomboid-like family members affects proteasome activity.

While it is not clear how microsomal proteasome activity is regulated by iRhom1, it is interesting to note that several assembly factors are detected in the microsomal fraction containing ER. In particular, large amounts of PAC1 and proteasomal subunits are consistently detected in the microsomal fraction. Moreover, a study in yeast showed that knockout of Pba2, a yeast homolog of PAC2, increases the accumulation and aggregation of misfolded proteins in the ER (Scott et al., 2007), consistent to our results. Accordingly, it has been reported that chymotrypsin-like activity is more critical for cell as functions in ER-associated cellular processes and affects sensitivity to stress-induced degradation of misfolded protein (Tomaru et al., 2012). I do not understand how overexpression of iRhom1 elevates only chymotrypsin-like activity, iRhom1, as an ER-resident protein, may regulate proteasome assembly through PACs in the ER. This idea is in a line with a report showing that the ER may be the subcellular organ in which proteasome assembly and activity are regulated (Fricke et al., 2007). From the fractionation assays following the protocol presented previously (Lim et al., 2009; Shim et al., 2011), I see high levels of proteasome activity in the microsomal fraction which contains ER and nuclear membranes. While it is known that proteasomes, in general, are localized largely in the cytosol and nucleus (Wojcik and DeMartino, 2003), more quantification for the proteasome activity in the ER fraction using diverse assays is needed.

It has been reported that *de novo* proteasome assembly can endure or overcome stressful conditions, such as oxidative stress, by increasing the transcription of proteasome subunits (Koch et al., 2011) or assembly chaperones (Chen et al., 2006). Similarly, it is reasonable to propose that proteasome assembly itself can be regulated to respond to stressful conditions through proteasome assembly factors, as previously shown by us in the case of S5b under chronic inflammation (Shim et al., 2012). Like Rpn4 which regulates the transcription of yeast proteasome subunits has an extremely short half-life and responds to various stress signals (Dohmen et al., 2007), I believe that PAC1 is regulated by iRhom1 to ensure the assembly of proteasomes under ER stress.

PAC1 and PAC2 form heterodimer and this dimerization increases their stability(Hirano et al., 2005). In our experiments, iRhom1 affected this heterodimerization and consequently the stability of PAC1 and PAC2 proteins. An important question that remains is, then, how iRhom1 regulates the stability of PAC1 and PAC2 proteins as well as their dimerization. HRD1, an E3 ubiquitin ligase in ERAD (Kanehara et al., 2010), binds to PAC1, and this interaction is regulated by iRhom1 in our assays (data not shown). Moreover, ectopic expression of HRD1 or a dominant-negative p97/VCP mutant potentiated the increase of proteasome activity by iRhom1 (data not shown). Considering that PAC1 and PAC2 are actively involved in the assembly of the 20S proteasome complex (Le Tallec et al., 2007), iRhom1

may regulate the stability of PAC1 and PAC2 proteins probably through HRD1.

ER stress is induced by diverse cellular stressors, including calcium overload, glucose deprivation, or malformed proteins such as non-glycosylated or damaged proteins. Most abnormal secretory proteins are destined for degradation by ERAD, thereby reducing the load on cellular homeostasis caused by ER stress(Meusser et al., 2005). From our experiments, I found that the proteasome activity in the ER-containing microsomal fraction is affected by ER stress. Then, how is the proteasome activity in the microsomal fraction selectively regulated under ER stress? As several unfolded protein response (UPR) and ERAD-related genes expression are induced to overcome the stress (Kaneko et al., 2007), the induction of iRhom1 at early stage of ER stress can be interpreted to function as a kind of ER stress sensor to regulate ER-associated proteasome activity. It has been noted that the Ufd-Npl4-p97/VCP protein complexes, which transports ERAD substrates from the ER to the cytosol, binds to the proteasome and this binding may recruit the proteasome to ERAD components (Wolf and Stolz, 2012). I also found that iRhom1 binds to p97/VCP as other rhomboid proteases do (Fleig et al., 2012); however, this binding affected neither proteasome assembly nor proteasome activity in our assays. It thus appears that the regulation of microsomal proteasome activity is not associated with ERAD machinery; rather, it is associated with PACs. On the other hand, proteasome

activity might be affected by additional signal as well as iRhom under the prolonged ER stress (Lee et al., 2010).

Consistent with the stimulatory role of iRhom1 in proteasome activation in cultured cells, iRhom1 is critical in the regulation of proteasome activity and in regulating the aggregation and neurotoxicity of mtHtt in *D. melanogaster*. Our results show a peculiar role of iRhom1 in the regulation of proteasome activity under ER stress. Because iRhom1 is a type of inspection protein for secretory proteins and a mediator in ER stress-associated proteasome activation, it is conceivable that this quality control system may be coupled with stress response. Considering that mtHtt also causes ER stress (Vidal et al., 2011), the novel role for iRhom1 in increasing the activity of proteasomes under ER stress warrants further attention and proteasome regulation via iRhom1 provides insight into protein quality control.

References

Adams, J. 2003. The proteasome: structure, function, and role in the cell. *Cancer treatment reviews*. 29 Suppl 1:3-9.

Adrain, C., M. Zettl, Y. Christova, N. Taylor, and M. Freeman. 2012. Tumor necrosis factor signaling requires iRhom2 to promote trafficking and activation of TACE. *Science (New York, N.Y.)*. 335:225-228.

Chen, Q., J. Thorpe, J.R. Dohmen, F. Li, and J.N. Keller. 2006. Ump1 extends yeast lifespan and enhances viability during oxidative stress: central role for the proteasome? *Free radical biology & medicine*. 40:120-126.

Christianson, J.C., and Y. Ye. 2014. Cleaning up in the endoplasmic reticulum: ubiquitin in charge. *Nature structural & molecular biology*. 21:325-335.

Ciechanover, A. 2005. Intracellular protein degradation: from a vague idea thru the lysosome and the ubiquitin-proteasome system

and onto human diseases and drug targeting. *Cell death and differentiation*. 12:1178-1190.

Crowe, E., C. Sell, J.D. Thomas, G.J. Johannes, and C. Torres. 2009. Activation of proteasome by insulin-like growth factor-I may enhance clearance of oxidized proteins in the brain. *Mechanisms of ageing and development*. 130:793-800.

Dohmen, R.J., I. Willers, and A.J. Marques. 2007. Biting the hand that feeds: Rpn4-dependent feedback regulation of proteasome function. *Biochimica et biophysica acta*. 1773:1599-1604.

Elsasser, S., M. Schmidt, and D. Finley. 2005. Characterization of the proteasome using native gel electrophoresis. *Methods in enzymology*. 398:353-363.

Fleig, L., N. Bergbold, P. Sahasrabudhe, B. Geiger, L. Kaltak, and M.K. Lemberg. 2012. Ubiquitin-dependent intramembrane rhomboid protease promotes ERAD of membrane proteins. *Molecular cell*. 47:558-569.

Freeman, M. 2009. Rhomboids: 7 years of a new protease family. *Seminars in cell & developmental biology*. 20:231-239.

Fricke, B., S. Heink, J. Steffen, P.M. Kloetzel, and E. Kruger. 2007. The proteasome maturation protein POMP facilitates major steps of 20S proteasome formation at the endoplasmic reticulum. *EMBO reports*. 8:1170-1175.

Godderz, D., and R.J. Dohmen. 2009. Hsm3/S5b joins the ranks of 26S proteasome assembly chaperones. *Molecular cell*. 33:415-416.

Greenblatt, E.J., J.A. Olzmann, and R.R. Kopito. 2011. Derlin-1 is a rhomboid pseudoprotease required for the dislocation of mutant alpha-1 antitrypsin from the endoplasmic reticulum. *Nature structural & molecular biology*. 18:1147-1152.

Groettrup, M., T. Ruppert, L. Kuehn, M. Seeger, S. Standera, U. Koszinowski, and P.M. Kloetzel. 1995. The interferon-gamma-inducible 11 S regulator (PA28) and the LMP2/LMP7 subunits govern the peptide production by the 20 S proteasome in vitro. *The Journal of biological chemistry*. 270:23808-23815.

Han, J., S. Jung, J. Jang, T.I. Kam, H. Choi, B.J. Kim, J. Nah, D.G. Jo, T. Nakagawa, M. Nishimura, and Y.K. Jung. 2014. OCIAD2 activates gamma-secretase to enhance amyloid beta production by interacting with nicastrin. *Cellular and molecular life sciences : CMLS*. 71:2561-2576.

Hebert, D.N., and M. Molinari. 2007. In and out of the ER: protein folding, quality control, degradation, and related human diseases. *Physiological reviews*. 87:1377-1408.

Heink, S., D. Ludwig, P.M. Kloetzel, and E. Kruger. 2005. IFN-gamma-induced immune adaptation of the proteasome system is an accelerated and transient response. *Proceedings of the National Academy of Sciences of the United States of America*. 102:9241-9246.

Hirano, Y., K.B. Hendil, H. Yashiroda, S. Iemura, R. Nagane, Y. Hioki, T. Natsume, K. Tanaka, and S. Murata. 2005. A heterodimeric complex that promotes the assembly of mammalian 20S proteasomes. *Nature*. 437:1381-1385.

Kanehara, K., W. Xie, and D.T. Ng. 2010. Modularity of the Hrd1 ERAD complex underlies its diverse client range. *The Journal of cell biology*. 188:707-716.

Kaneko, M., S. Yasui, Y. Niinuma, K. Arai, T. Omura, Y. Okuma, and Y. Nomura. 2007. A different pathway in the endoplasmic reticulum stress-induced expression of human HRD1 and SEL1 genes. *FEBS letters*. 581:5355-5360.

Kim, M., H.S. Lee, G. LaForet, C. McIntyre, E.J. Martin, P. Chang, T.W. Kim, M. Williams, P.H. Reddy, D. Tagle, F.M. Boyce, L. Won, A. Heller, N. Aronin, and M. DiFiglia. 1999. Mutant huntingtin expression in clonal striatal cells: dissociation of inclusion formation and neuronal survival by caspase inhibition. *The Journal of neuroscience : the official journal of the Society for Neuroscience*. 19:964-973.

Koch, A., J. Steffen, and E. Kruger. 2011. TCF11 at the crossroads of oxidative stress and the ubiquitin proteasome system. *Cell cycle (Georgetown, Tex.)*. 10:1200-1207.

Le Tallec, B., M.B. Barrault, R. Courbeyrette, R. Guerois, M.C. Marsolier-Kergoat, and A. Peyroche. 2007. 20S proteasome assembly is orchestrated by two distinct pairs of chaperones in yeast and in mammals. *Molecular cell*. 27:660-674.

Lee, H., J.Y. Noh, Y. Oh, Y. Kim, J.W. Chang, C.W. Chung, S.T. Lee, M. Kim, H. Ryu, and Y.K. Jung. 2012. IRE1 plays an essential role in ER stress-mediated aggregation of mutant huntingtin via the inhibition of autophagy flux. *Human molecular genetics*. 21:101-114.

Lee, S.H., Y. Park, S.K. Yoon, and J.B. Yoon. 2010. Osmotic stress inhibits proteasome by p38 MAPK-dependent phosphorylation. *The Journal of biological chemistry*. 285:41280-41289.

Lee, W.C., M. Yoshihara, and J.T. Littleton. 2004. Cytoplasmic aggregates trap polyglutamine-containing proteins and block axonal transport in a Drosophila model of Huntington's disease. *Proceedings of the National Academy of Sciences of the United States of America*. 101:3224-3229.

Li, X., C.E. Wang, S. Huang, X. Xu, X.J. Li, H. Li, and S. Li. 2010. Inhibiting the ubiquitin-proteasome system leads to preferential accumulation of toxic N-terminal mutant huntingtin fragments. *Human molecular genetics*. 19:2445-2455.

Lim, P.J., R. Danner, J. Liang, H. Doong, C. Harman, D. Srinivasan, C. Rothenberg, H. Wang, Y. Ye, S. Fang, and M.J. Monteiro. 2009. Ubiquilin and p97/VCP bind erasin, forming a complex involved in ERAD. *The Journal of cell biology*. 187:201-217.

McIlwain, D.R., P.A. Lang, T. Maretzky, K. Hamada, K. Ohishi, S.K. Maney, T. Berger, A. Murthy, G. Duncan, H.C. Xu, K.S. Lang, D. Haussinger, A. Wakeham, A. Itie-Youten, R. Khokha, P.S. Ohashi, C.P. Blobel, and T.W. Mak. 2012. iRhom2 regulation of TACE controls TNF-mediated protection against Listeria and responses to LPS. *Science (New York, N.Y.)*. 335:229-232.

Meusser, B., C. Hirsch, E. Jarosch, and T. Sommer. 2005. ERAD: the long road to destruction. *Nature cell biology*. 7:766-772.

Murata, S., K. Sasaki, T. Kishimoto, S. Niwa, H. Hayashi, Y. Takahama, and K. Tanaka. 2007. Regulation of CD8+ T cell

development by thymus-specific proteasomes. *Science (New York, N.Y.)*. 316:1349-1353.

Noh, J.Y., H. Lee, S. Song, N.S. Kim, W. Im, M. Kim, H. Seo, C.W. Chung, J.W. Chang, R.J. Ferrante, Y.J. Yoo, H. Ryu, and Y.K. Jung. 2009. SCAMP5 links endoplasmic reticulum stress to the accumulation of expanded polyglutamine protein aggregates via endocytosis inhibition. *The Journal of biological chemistry*. 284:11318-11325.

Possik, P.A., C.A. Sommer, J. Issa Hori, G.M. Machado-Santelli, M.C. Jamur, and F. Henrique-Silva. 2004. DSCR2, a Down syndrome critical region protein, is localized to the endoplasmic reticulum of mammalian cells. *European journal of histochemistry : EJH*. 48:267-272.

Scott, C.M., K.B. Kruse, B.Z. Schmidt, D.H. Perlmutter, A.A. McCracken, and J.L. Brodsky. 2007. ADD66, a gene involved in the endoplasmic reticulum-associated degradation of alpha-1-antitrypsin-Z in yeast, facilitates proteasome activity and assembly. *Molecular biology of the cell*. 18:3776-3787.

Shim, S., W. Lee, H. Chung, and Y.K. Jung. 2011. Amyloid beta-induced FOXRED2 mediates neuronal cell death via inhibition of proteasome activity. *Cellular and molecular life sciences : CMLS*. 68:2115-2127.

Shim, S.M., W.J. Lee, Y. Kim, J.W. Chang, S. Song, and Y.K. Jung. 2012. Role of S5b/PSMD5 in proteasome inhibition caused by TNF-alpha/NFkappaB in higher eukaryotes. *Cell reports*. 2:603-615.

Steffen, J., M. Seeger, A. Koch, and E. Kruger. 2010. Proteasomal degradation is transcriptionally controlled by TCF11 via an ERAD-dependent feedback loop. *Molecular cell*. 40:147-158.

Stone, H.R., and J.R. Morris. 2014. DNA damage emergency: cellular garbage disposal to the rescue? *Oncogene*. 33:805-813.

Tanahashi, N., Y. Murakami, Y. Minami, N. Shimbara, K.B. Hendil, and K. Tanaka. 2000. Hybrid proteasomes. Induction by interferon-gamma and contribution to ATP-dependent proteolysis. *The Journal of biological chemistry*. 275:14336-14345.

Tomaru, U., S. Takahashi, A. Ishizu, Y. Miyatake, A. Gohda, S. Suzuki, A. Ono, J. Ohara, T. Baba, S. Murata, K. Tanaka, and M. Kasahara. 2012. Decreased proteasomal activity causes age-related phenotypes and promotes the development of metabolic abnormalities. *The American journal of pathology*. 180:963-972.

Vidal, R., B. Caballero, A. Couve, and C. Hetz. 2011. Converging pathways in the occurrence of endoplasmic reticulum (ER) stress in Huntington's disease. *Current molecular medicine*. 11:1-12.

Wojcik, C., and G.N. DeMartino. 2003. Intracellular localization of proteasomes. *The international journal of biochemistry & cell biology*. 35:579-589.

Wolf, D.H., and A. Stolz. 2012. The Cdc48 machine in endoplasmic reticulum associated protein degradation. *Biochimica et biophysica acta*. 1823:117-124.

Xu, S., G. Peng, Y. Wang, S. Fang, and M. Karbowski. 2011. The AAA-ATPase p97 is essential for outer mitochondrial membrane protein turnover. *Molecular biology of the cell*. 22:291-300.

Yan, Z., H. Zou, F. Tian, J.R. Grandis, A.J. Mixson, P.Y. Lu, and L.Y. Li. 2008. Human rhomboid family-1 gene silencing causes apoptosis or autophagy to epithelial cancer cells and inhibits xenograft tumor growth. *Molecular cancer therapeutics*. 7:1355-1364.

Yoshida, Y., and K. Tanaka. 2010. Lectin-like ERAD players in ER and cytosol. *Biochimica et biophysica acta*. 1800:172-180.

Zettl, M., C. Adrain, K. Strisovsky, V. Lastun, and M. Freeman. 2011. Rhomboid family pseudoproteases use the ER quality control machinery to regulate intercellular signaling. *Cell*. 145:79-91.

Zhou, Z., F. Liu, Z.S. Zhang, F. Shu, Y. Zheng, L. Fu, and L.Y. Li. 2014. Human rhomboid family-1 suppresses oxygen-independent degradation of hypoxia-inducible factor-1alpha in breast cancer. *Cancer research*. 74:2719-2730.

CHPATER II

S5b induces neuronal cell death via downregulation of GRK2

Abstract

S5b was identified as a proteasome-assembly chaperone in yeast and a negative regulator of 26S proteasome in mammalian. Regulation of GRK2 is considered as one of cell death mediators in neuronal cells. However, the regulation of GRK2 expression is not known. Here, I show that GRK2 is regulated by S5b in neuronal cells and mouse model. GRK2 is down-regulated in the cortex and hippocampus of S5b transgenic mice, a chronic inflammation model and also reduced by S5b expression in HT22 mouse hippocampal cells. Conversely, knockdown of S5b expression increases GRK2 level through increasing the stability of GRK2 protein. This activity of S5b is not associated with its ability to impair proteasome activity. S5b and S5b K220R mutant similarly interacts with GRK2 in the mouse cortex and HT22 cells through its C-terminal domain. Overexpression of S5b C-terminal domain also decreases GRK2 level. Membrane targeting of GRK2 is also affected by S5b expression, as assessed with immunocytochemistry, fractionation, and surface biotinylation assays. In addition, neurotoxic effect of S5b is suppressed by overexpression of GRK2 but not by GRK2 K220R, a kinase dead mutant. Thus, S5b may exert its toxic effect through down-regulation of GRK2, a neurotoxic mediator, in neuronal cells, showing an aberrant role of S5b as a negative regulator of GRK2 in neuronal cell death.

In addition, *Psmd5*/S5b knockout mouse was successfully generated by the Cas9/CRISPR-mediated PSMD5/S5b knockout cassette and show enhanced proteasome activity compared to aged matched littermates. Together, S5b plays a diverse role in the regulation of proteasome activity under pathologic condition and in neuronal cell death through GRK2.

Introduction

S5b was first discovered as a proteasome subunit together with S5a (Deveraux, Jensen and Rechsteiner, 1995). Recently, S5b was identified as a 19S protasome assembly chaperone with PAAF1, p27, and p28 in yeast (Funakoshi et al., 2009; Park et al., 2009; Roelofs and Finley, 2009; Saeki et al., 2009). S5b forms a proteasome subcomplex via interaction with S7, S4, and S2 proteasome subunits (Gorbea et al., 2000). Deletion of chaperones in yeast is not lethal in normal condition except S5b (Funakoshi et al., 2009; Park et al., 2009; Roelofs and Finley, 2009; Saeki et al., 2009). The absence of the S5b leads to severe growth and proteasome assembly defects (Saeki et al., 2009). However, function of S5b seems to be different in mammalian cells and animals. Unlike in yeast, overexpression of S5b induces proteasome disassembly and inhibition, showing early aging phenotype, including short life span in mice (Barrault et al., 2012; Shim et al., 2012). Deletion of S5b alleviates tauopathy phenotype and expands life span in fly via up-regulation of proteasome activity (Barrault et al., 2012). S5b is also induced by inflammatory signal, such as TNF-α and IL-1β, but downstream or binding partner of S5b is not well understood.

G-protein-coupled receptors (GPCRs) comprise the largest known family of cell-surface receptors and are fundamentally involved in diverse

mammalian physiology (Ribas et al., 2007; Penela et al., 2010). This receptor superfamily represents the largest single target for drug therapy (Ribas et al., 2007) and GPCR dysfunction/dysregulation is a major contributor to the pathophysiology of diseases (Harris et al., 2008; Obrenovich et al., 2009). The GRKs are serine/threonine protein kinases that phosphorylate GPCR in an agonist-dependent manner, resulting in homologous desensitization of the receptor (Liggett, 2011). Phosphorylation of β-adrenergic receptor, one of the GPCR, by GRK2 promotes recruiting of β-arrestins from cytosol to membrane, and stimulates receptor desensitization and internalization (Whalen et al., 2007). GRK2 protein expression is reduced in immune cells during the acute phase of adjuvant arthritis in the rat as well as during relapsing progressive experimental autoimmune encephalomyelitis (EAE) (Vroon et al., 2007). Although GRK2 is critical for the desensitization of GPCRs and for immune response, regulatory mechanism of GRK2 is not well understood.

In my results, I identified novel function of S5b irrelevant to its ability to regulate proteasome activity. I show that overexpressed S5b interacts with GRK2 and reduces the expression level and membrane targeting of GRK2, which contributes to neuronal cell death.

Materials and Methods

Material

The following antibodies were used: anti-GFP, anti-Tubulin, anti-HA, anti-Actin, anti-GRK2, anti-S5b, anti-PARP-1, anti-Caspase-3, anti-Caspase9 (SantaCruz); anti-GFAP, anti-MAP2 (Millipore); and anti-DR5 (Abcam). IDN-6556 was purchased from Sigma-Aldrich. Ethidium homodimer was purchased from Molecular Probes. GRK2 siRNA was purchased from bioneer**.** S5b Tg mice, GFP-S5b deletion mutants and S5b shRNAs were generated as previously described (8).

Cell Culture and DNA Transfection

HEK293T and other cells were obtained from the American Type Culture Collection (ATCC) and grown in DMEM or RPMI containing 10% fetal bovine serum and penicillin/streptomycin at 37°C under 5% CO_2 (v/v). Cells were transfected with the appropriate vectors using Lipofectamine and Lipofectamine 2000 reagents (Invitrogen) according to the manufacturer's instructions.

SDS-PAGE and Immunoblot Analysis

Protein samples were prepared in rectic buffer (30 mM Tris pH 7.8, 5 mM $MgCl_2$, 10 mM KCl, 0.5% TritonX-100, and protease inhibitor cocktail) by sonication and centrifuged at 12,000 rpm at 4 ºC for 10 min. Supernatants were subjected to SDS-PAGE and resolved proteins were transferred onto nitrocellulose membranes using a BioRad semi-dry transfer unit. Blots were blocked with 3 % (w/v) non-fat dry milk in TBS-T solution [25 mM Tris pH 7.5, 150 mM NaCl, and 0.05 % (w/v) Tween-20]. After washing with TBS-T, blots were incubated with primary antibodies, followed by horseradish peroxidase-conjugated secondary antibodies. Immunoreactive bands were detected by ECL reagents.

Immunoprecipitation and Immunohistochemisty

Cell lysates were prepared by sonication using rectic buffer and then centrifuged at 12,000 rpm for 30 min at 4℃. The supernatants were incubated with primary antibody and pulled down by Protein G sepharose beads (GE Healthcare). Immunostaing of mouse brain was examined by cresyl violet and indicated antibodies, as previously described (Vitner et al., 2012).

Subcellular Fractionation

Cells were resuspended in buffer (20 mM HEPES pH 7.5, 10 mM KCl, 1.5 mM $MgCl_2$, 1 mM EDTA, and 1 mM phenylmethylsulphonyl fluoride), and

incubated on ice for 20 min in the presence of 250 mM sucrose. Cell lysates were centrifuged at 1,000*g* for 5 min at 4 °C, and the supernatant was further centrifuged at 8,000*g* for 20 min at 4 °C. The supernatant was further centrifuged at 100,000*g* for 3 h at 4 °C. The resulting pellet retained the microsomal fraction, whereas the supernatant contained cytosol.

Biotinylation assay

Cell lysates were washed with ice-cold PBS and incubated with Sulfo-NHS-SS-Biotin (Pierce biotechnology, 0.15 mg/ml) for 1 h at 4 °C. After washing cells with ice-cold PBS containing glycine to remove non-reacted biotinylation reagent, cells were lyzed in ice-cold RIPA buffer. After centrifugation (16,000g for 15 min at 4 °C), supernatants containing equal amount of protein were incubated with streptavidin beads to immunoprecipitate the remaining biotinylated proteins. The immunocomplexes were collected by centrifugation at 5,000 rpm for 3 min, washed with lysis buffer, and detected by western blotting, as described above.

Results

GRK2 level is regulated by S5b in HT22 cells and the brain of S5b transgenic mice

In the previous study, *Psmd5*/S5b transgenic (Tg) mouse was generated as a model of chronic inflammation model and show reduced proteasome activity in all tissues of the mice (Shim et al., 2012). During the characterization of the mouse phenotype, I found that the expression of GRK2 was significantly reduced in the cortex and hippocampus, but not in the cerebellum and striatum, of 3-month-old S5b Tg mice. Endogenous S5b and exogenous S5b-HA were ubiquitously expressed with similar level in all tissues examined (Figure II-1 A). When I examined the expression level during aging, I found that compared to age-matched littermates, GRK2 level was apparently reduced in the cortex and hippocampus of 3- to 12-month-old S5b Tg mice (Figure II-1 B).

I also analyzed this regulation in HT22 mouse hippocampal cell line. Ectopic expression of S5b reduced GRK2 level in a dose- and time-dependent manner in HT22 cells (Figure II-2 A.), consistent with the results from the mouse tissues. To examine whether S5b affects the stability of GRK2 protein, I checked the half-life of GRK2 protein after the treatment with cycloheximide, an inhibitor of protein translation. Quantification of the signal

intensity following western blot analysis revealed that the half-life of GRK2 protein was longer than 24 h in HT22 cells, but decreased to 6 h by S5b overexpression (Figure II-2 B).

I then examined the knockdown effect of S5b expression on GRK2 level by using shRNA. I found that knockdown of S5b expression increased GRK2 level in HT22 cells (Figure II-3 A). Similarly, western blot analysis using cycloheximide revealed that the half-life of GRK2 protein markedly increased to more than 36 h by S5b knockdown (Figure II-3 B). Together with the results from overexpression analysis, these results suggest that GRK2 expression is regulated by S5b.

S5b interacts with GRK2 through its C-terminus

To examine the mechanism by which S5b regulates GRK2 protien, I first checked the interaction of S5b with GRK2. The results from immunoprecipitation assay revealed that endogenous S5b was found in the endogenous GRK2-containing immunocomplex in the cortex of S5b Tg mice (Figure II-4 A, left) and HT22 cells (Figure II-4 A), indicating that S5b interacts with GRK2. Because it was previously reported that S5b interacts with S7 to impair proteasome activity through Arg184 residue, the mutation in S5b Arg184 residue loses the inhibitory function (Shim et al., 2012).

Thus, I explored the contribution of Arg184 residue of S5b to the destabilization of and interaction with GRK2. Western blot analysis showed

that the expression of S5b R184E mutant also reduced GRK2 level as much as wild-type S5b in the transfected cells (Figure II-4 B, left). In addition, immunoprecipitation assay showed that GRK2 equally interacted with both wild-type S5b and S5b R184E (Figure II-4 B). These results raise a possibility that S5b exerts its activity to destabilize GRK2 in a proteasome activity-independent manner.

Next, I decided to identify the S5b domain that interacts with GRK2 and impairs the protein stability of GRK2. I performed immunoprecipitation analysis using S5b deletion mutants lacking the C- or N-terminus (Shim et al., 2012), (Figure II-4 D). The results indicate that only S5b C1 mutant among S5b deletion mutants interacted with GRK2 (Fig. II-4 C, middle and right) and this pattern of the interaction differs from the binding of S5b with S7 (Shim et al., 2012), Consistently, only S5b C1 mutant reduced GRK2 level as much as wild-type S5b (Fig. II-4 C, left). The observations suggest that the interaction between S5b and GRK2 may be critical for the regulation of GRK2 level.

S5b impairs the targeting of GRK2 to the plasma membrane

GRK2 is a cytosolic protein that is often recruited to the plasma membrane for desensitizing the receptors (Cong et al., 2001) and for negative feedback regulatory mechanism (Cannavo et al., 2013). When I assessed GRK2 translocation using immunocytochemical analysis, I found that GRK2

was located in the cytosol and plasma membrane in control cells. Interestingly, overexpression of S5b decreased the targeting of GRK2 to the plasma membrane but increased its cytosol distribution, increasing its colocalization with S5b in the cytosol (Figure II-5 A).

I further analyzed this change of subcellular localization of GRK2 using fractionation assay. HT22 cell extracts were separated into the membrane fraction and the cytosolic fraction using centrifugation. Western blotting of the fractions revealed that GRK2 was equally found in the both cytosol and membrane fractions in control cells, while S5b was detected exclusively in the cytosolic fraction. On the other hand, ectopic expression of S5b reduced the amount of GRK2 in the membrane fraction (Figure II-6 A). Tubulin and DR5 were utilized as marker proteins of cytosol and a membrane, respectively (Figure II-6 A). These indicate that membrane localization of GRK2 is also regulated by S5b.

I further assessed GRK2 translocation by S5b using biotinylation assay. The results show that GRK2 was detected by pull-down assay using streptavidin, while S5b was not detected. DR5 was used as a loading control in the assay (Figure II-6 B). Consistently, the level of biotinylated GRK2 detected by pull-down assay using streptavidin decreased by S5b overexpression but increased by S5b knockdown in HT 22 cells (Figure II-6 B). These results suggest that expression level of S5b is important to affect not only the level of GRK2 protein but also its membrane translocation.

S5b affects neuronal cell death probably via down-regulation of GRK2

Since GRK2 has a neuroprotective role, I assessed the relation of S5b-induced down-regulation of GRK2 to neuronal cell death. Since S5b is induced during chronic inflammation and toxic to the cells (Shim et al., 2012), I directly addressed their overexpression effects on cell death. As expected, ectopic expression of S5b induced significant amount of cell death at 24 h in HT22 cells, while S5b knockdown alone did not affect cell death (Figure II-7 A). PARP-1 cleavage and caspase-9 activation were evidently observed by S5b expression (Figure II-7 B). As expected, knockdown of GRK2 expression with siRNA also induced significant cell death in a dose-dependent manner (Figure II-8 A). Interestingly, S5b-induced cell death was suppressed by overexpression of GRK2 but not by GRK2 K220R mutant which loses its kinase activity (Figure II-8 B). Collectively, these results suggest that the neurotoxic effect of S5b might be mediated through down-regulation of GRK2.

Generation of *Psmd5*/S5b knockout mice with enhanced proteasome activity

To further determine the effect of S5b knockout on GRK2 level and proteasome activity *in vivo*, *Psmd5*/S5b knockout mice were generated by utilizing Cas9/CRISPR system by injecting a transcript, encoding Cas9 transgene expression cassette into the embryonic stem (ES) cells (Figure II-9

A). After screening several mouse lines, I found 3 lines of S5b knockout mice whose exon 2 was targeted. From genomic sequencing analysis of the PCR products, I found alleles of these mice with various deletions with frame shift. As a genotype marker, common restriction enzyme site *Bsu36I*, which cuts wild-type S5b but not deletion mutant, was employed to distinguish the deletion mutants from wild-type in their genome. As a result, I isolated S5b knockout mice whose DNA was not cut by this enzyme and had frame shift mutation (Figure II-9 B).

Next, I established *Psmd5*$^{-/-}$ mouse after several times of its cross with wild-type mice. After 3 passages, I isolated *Psmd5*$^{-/-}$ mouse and then examined the expression pattern of S5b. Western blotting analysis revealed that the level of S5b protein in one-month-old *Psmd5*$^{-/-}$ mouse was lost in the peripheral tissues, including liver, lung, kidney and spleen, and brain subregions, such as cortex, hippocampus and cerebellum (Figure II-10 A and B). Interestingly, this mouse also showed reduced level of p53 which is known as a proteasome substrate (Figure II-10 A). Therefore, I measured proteasome activity using fluorogenic substrates. More interestingly, proteasome catalytic activity in the tissue extracts was significantly elevated in almost all of the tissues we examined (Figure II-11 A and B). In addition, GRK2 level in the brain of one-month-old *Psmd5*$^{-/-}$ mouse was not much changed yet.

Figure II-1. GRK2 is down-regulated in the cortex and hippocampus of S5b transgenic mice. (**A**) Tissue extracts of brain subsection (cortex, hippocampus, striatum, cellebellum, brain stem, and olfactory bulb) and heart were prepared from 3-month-old wild-type (WT) or S5b Tg mice and analyzed by Western blot analyses (top). Signals on the blots were quantified using densitometry analysis. GRK signal was normalized by Actin and relative ratios of GRK signal in S5b TG mice to WT mice are indicated (bottom). (**B**) Cortical (top) and hippocampal (bottom) tissues were collected from 3-, 6-, 9-, and 12-month-old S5b Tg mice and their littermate, and tissue extracts were analyzed with Western blotting.

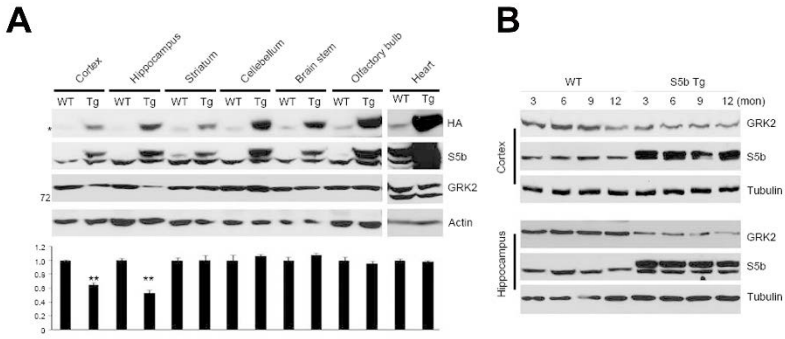
A
Cortex
Hippocampus
Striatum
Cellebellum
Brain stem
Olfactory bulb
Heart
WT Tg WT Tg WT Tg WT Tg WT Tg WT Tg WT Tg
HA
S5b
GRK2
Actin
72
1.2
1.0
0.8
0.6
0.4
0.2
0
**
**
B
WT
S5b Tg
3 6 9 12 3 6 9 12 (mon)
Cortex
GRK2
S5b
Tubulin
Hippocampus
GRK2
S5b
Tubulin

Figure II-2. GRK2 is down-regulated by the ectopic expression of S5b in HT22 hippocampal cells. (**A**) HT22 cells were transfected with pcDNA or S5b for 36 h (left) or for the indicated times (right). Cell extracts were prepared and analyzed by Western blotting. (**B**) After being transfected for 24 h with EGFP or GFP-S5b, cells were exposed to 30 μg/ml cycloheximide (CHX) for the indicated times and analyzed by with Western blotting (left). Signals on the blots were quantified using densitometry analysis and relative ratios of GRK signal to control (time 0) (GRK2/Actin) are indicated (right).

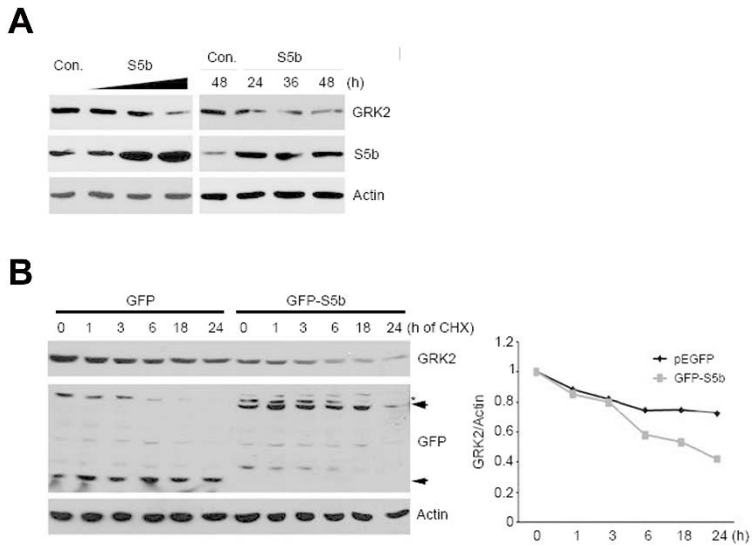
A
Con.
S5b
Con.
S5b
48 24 36 48 (h)
GRK2
S5b
Actin
B
GFP
GFP-S5b
0 1 3 6 18 24 0 1 3 6 18 24 (h of CHX)
GRK2
GFP
Actin
GRK2/Actin
1.2
1
0.8
0.6
0.4
0.2
0
pEGFP
GFP-S5b
0 1 3 6 18 24 (h)

Figure II-3. Knockdown of S5b expression increases GRK2 at the post-transcription level. (**A**) HT22 cells were transfected for 48 h with pcDNA, S5b shRNA#2, or S5b shRNA#5 and cell extracts were examined with Western blot analyses. (**B**) After being transfected for 24 h with pSUPER or S5b shRNA, HT22 cells were exposed to 30 μg/ml cycloheximide (CHX) for the indicated times, after which cell extracts were examined by Western blot analyses (left). Signals on the blot were quantified using densitometry analysis. GRK signal was normalized by Actin and their relative ratios to control (time 0) are indicated (right).

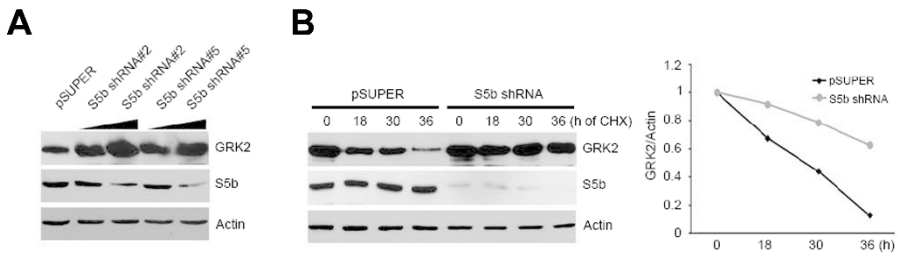
A
pSUPER
S5b shRNA#2
S5b shRNA#2
S5b shRNA#5
S5b shRNA#5
GRK2
S5b
Actin
B
pSUPER
S5b shRNA
0 18 30 36 0 18 30 36 (h of CHX)
GRK2
S5b
Actin
GRK2/Actin
1.2
1
0.8
0.6
0.4
0.2
0
pSUPER
S5b shRNA
0 18 30 36 (h)

Figure II-4. S5b interacts with GRK2 through its C-terminal domain.

(**A**) Cortical tissue (left) and HT22 cell extracts (right) were prepared and subjected to immunoprecipitation (IP) analyses using preimmune serum (Pre), anti-S5b, or anti-GRK2 antibody. Whole tissue or cell lysates (WCL) and the immunoprecipitates were analyzed with Western blotting. (**B**) HEK293T cells were transfected with pcDNA, HA-S5b (WT), or HA-S5b R184E (RE) for 36 h and cell lysates were subjected to an IP assay using anti-GRK2 or anti-HA antibody. (**C**) HEK293T cells were transfected with GFP-tagged S5b deletion mutants for 36 h, and immunoprecipitation (IP) assays were performed with anti-GFP (middle) or anti-GRK2 (right) antibody. Total cell lysates (WCL) (left) and the immunoprecipitates (IP) (middle and right) were analyzed by Western blotting. (**D**) Schematic diagram of S5b deletions and summary of the interaction.

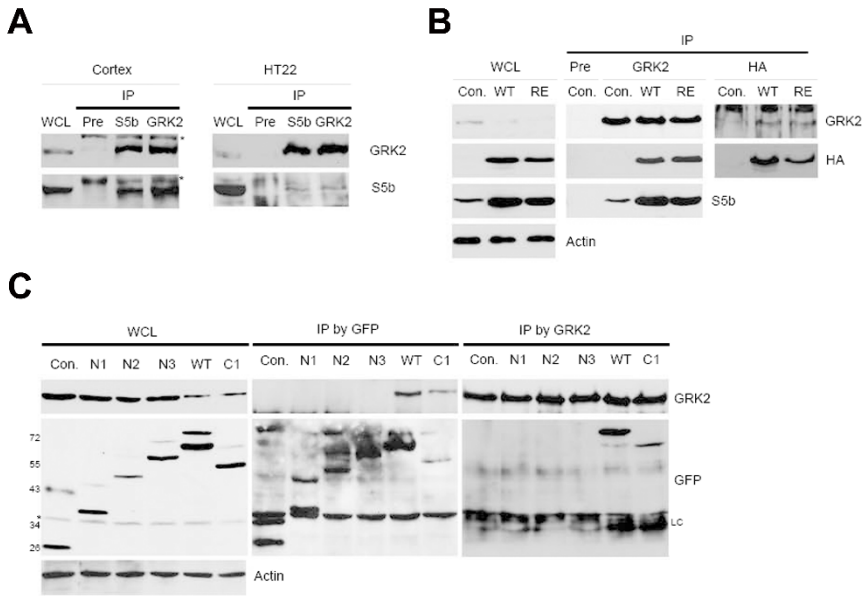
A
Cortex
HT22
IP
IP
WCL Pre S5b GRK2
WCL Pre S5b GRK2
GRK2
S5b
B
IP
WCL
Pre GRK2 HA
Con. WT RE
Con. Con. WT RE
Con. WT RE
GRK2
HA
S5b
Actin
C
WCL
IP by GFP
IP by GRK2
Con. N1 N2 N3 WT C1
Con. N1 N2 N3 WT C1
Con. N1 N2 N3 WT C1
GRK2
GFP
LC
72
55
43
34
26
Actin
D
Amino Acid
Interaction with S7
Interaction with GRK2
Proteasome inhibition
WT 1-504 + + +
N1 1-153 – – –
N2 1-328 + – –
N3 1-432 + – +
C1 154-504 + + –
R184 : S7 interaction site

Figure II-5. Translocation of GRK2 to the cytosol by S5b expression. (**A**) HT22 cells were transfected with EGFP, GFP-S5b, or both S5b shRNA and EGFP for 48 h and then subjected to immunostaining analysis with anti-GRK2 antibody (*red*).

A

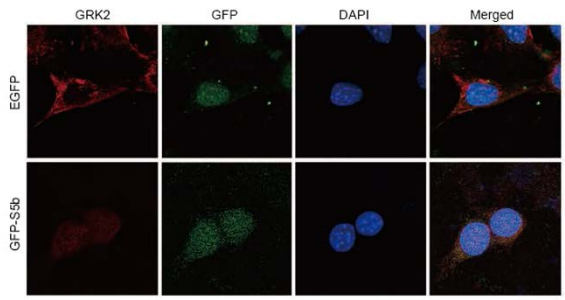

Figure II-6. S5b recruits membrane GRK2 into the cytosol. (**A)** HT22 cells were transfected with pcDNA, S5b, or S5b shRNA for 48 h and cytosolic (C) and membrane (M) fractions were then prepared by centrifugation as described in ***Materials*** and Methods. Each fraction was separated by SDS-PAGE and analyzed by Western blotting (left). The signals on the blots were quantified by densitometry analysis (right). Bars represent mean values ± SD. (**B**) HT22 cells were transfected with pcDNA, S5b, or S5b shRNA for 48 h and then biotinylation assays were performed as described in the ***Materials*** and Methods.

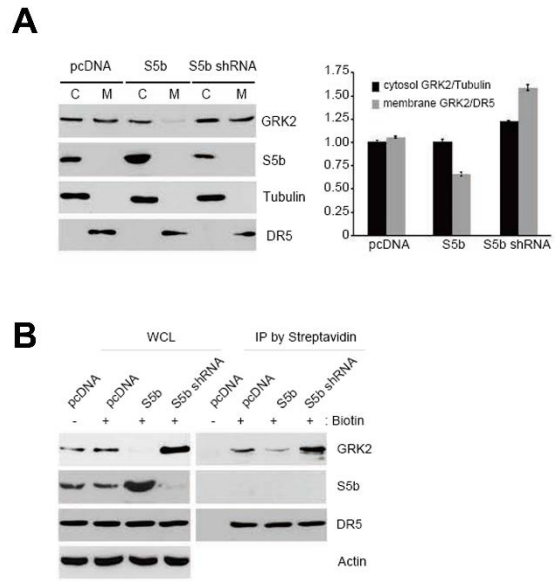
A
pcDNA
S5b
S5b shRNA
C M C M C M
GRK2
S5b
Tubulin
DR5
cytosol GRK2/Tubulin
membrane GRK2/DR5
1.75
1.50
1.25
1.00
0.75
0.50
0.25
0
pcDNA
S5b
S5b shRNA
B
WCL
IP by Streptavidin
pcDNA
pcDNA
S5b
S5b shRNA
pcDNA
pcDNA
S5b
S5b shRNA
- + + + - + + + : Biotin
GRK2
S5b
DR5
Actin

Figure II-7. Over-expressed S5b induces apoptosis in HT22 cells. (**A**) HT22 cells were cotransfected with EGFP and pcDNA, S5b, or S5b shRNA for 24 h or 48 h and cell death was then examined using ethidium homodimer staining. Cell lysates were analyzed by Western blotting (insert). (**B**) HT22 cells were transfected with EGFP or EGFP-S5b in the absence or presence of 10 μM IDN6556 and cell lysates were analyzed by Western blotting.

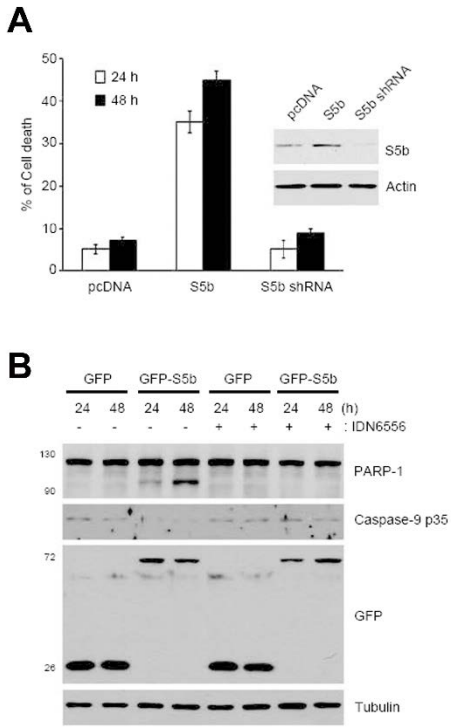
A
50
40
30
20
10
0
% of Cell death
24 h
48 h
pcDNA
S5b
S5b shRNA
pcDNA
S5b
S5b shRNA
S5b
Actin
B
GFP
GFP-S5b
GFP
GFP-S5b
24 48 24 48 24 48 24 48 (h)
- - - - + + + + : IDN6556
130
90
72
26
PARP-1
Caspase-9 p35
GFP
Tubulin

Figure II-8. GRK2 suppresses S5b-induced cell death in an activity-dependent manner. (**A**) After co-transfection of HT22 cells with EGFP and GRK2 siRNA for 48 h, cell death was examined using ethidium homodimer staining (left) and cell lysates were analyzed by Western blotting (right). (**B**) HT22 cells were co-transfected with GFP- S5b and GRK2 WT or GRK2 K220R (KR) mutant for 48 h and cell death was then examined after staining with ethidium homodimer (top). Cell lysates were analyzed by Western blotting (bottom). In all panels, bars represent mean values ± SD.

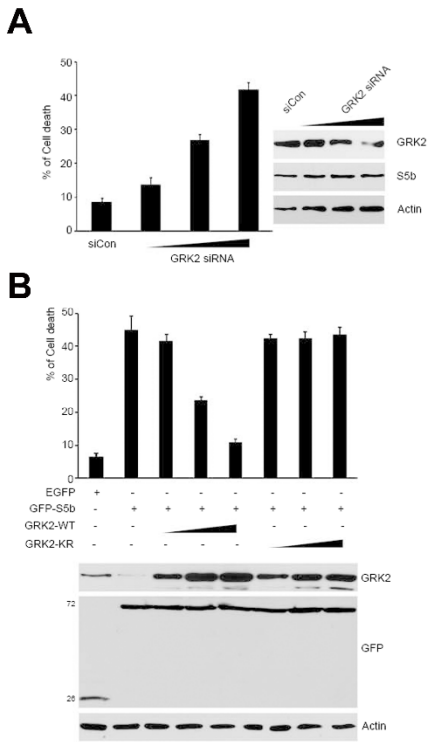
A
% of Cell death
50
40
30
20
10
0
siCon
GRK2 siRNA
siCon
GRK2 siRNA
GRK2
S5b
Actin
B
% of Cell death
50
40
30
20
10
0
EGFP + - - - - - - -
GFP-S5b - + + + + + + +
GRK2-WT - - - - - - -
GRK2-KR - - - - - - -
GRK2
72
GFP
26
Actin

Figure II-9 Generation of PSMD5/S5b knockout mice by Cas9/CRISPR. (**A**) Schematic diagram of the Cas9/CRISPR-mediated PSMD5/S5b knockout cassette. (**B**) Genome sequencing of exon 2 mutation in *Psmd5* knockout mice (upper). Four week-old mice tails were harvested, and solved DirectPCR Lysis Reagent for overnight in 65℃ and tail DNA (100 ng) was then analyzed by genomic PCR. The PCR products were digested with *Bsu36I* and analyzed with 1.5% agrose gel electrophoresis (lower).

A

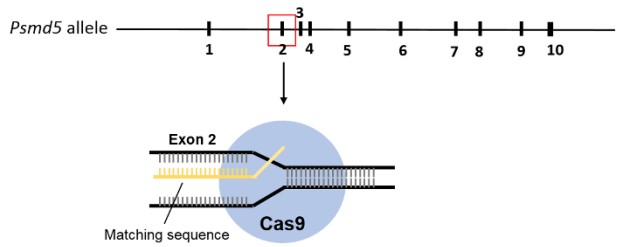
Psmd5 allele
1
2
3
4
5
6
7
8
9
10
Exon 2
Cas9
Matching sequence

B

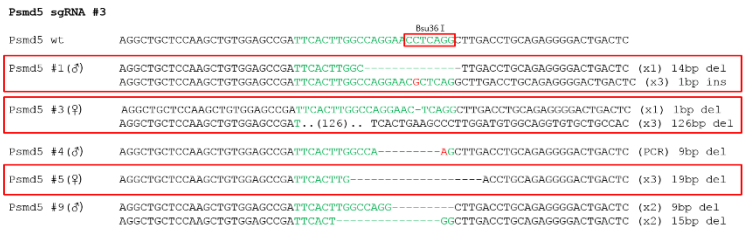
Psmd5 sgRNA #3
8su36 I
Psmd5 wt AGGCTGCTCCAAGCTGTGGAGCCGATTCACTTGGCCAGGAACCTCAGGCTTGACCTGCAGAGGGGACTGACTC
Psmd5 #1(♂) AGGCTGCTCCAAGCTGTGGAGCCGATTCACTTGGC----------TTGACCTGCAGAGGGGACTGACTC (x1) 14bp del
AGGCTGCTCCAAGCTGTGGAGCCGATTCACTTGGCCAGGAACGCTCAGGCTTGACCTGCAGAGGGGACTGACTC (x3) 1bp ins
Psmd5 #3(♀) AGGCTGCTCCAAGCTGTGGAGCCGATTCACTTGGCCAGGAAC-TCAGGCTTGACCTGCAGAGGGGACTGACTC (x1) 1bp del
AGGCTGCTCCAAGCTGTGGAGCCGAT..(126).. TCACTGAAGCCCTTGGATGTGGCAGGTGTGCTGCCAC (x3) 126bp del
Psmd5 #4(♂) AGGCTGCTCCAAGCTGTGGAGCCGATTCACTTGGCCA---------AGCTTGACCTGCAGAGGGGACTGACTC (PCR) 9bp del
Psmd5 #5(♀) AGGCTGCTCCAAGCTGTGGAGCCGATTCACTTG----------ACCTGCAGAGGGGACTGACTC (x3) 19bp del
Psmd5 #9(♂) AGGCTGCTCCAAGCTGTGGAGCCGATTCACTTGGCCAGG---------CTTGACCTGCAGAGGGGACTGACTC (x2) 9bp del
AGGCTGCTCCAAGCTGTGGAGCCGATTCACT----------GGCTTGACCTGCAGAGGGGACTGACTC (x2) 15bp del

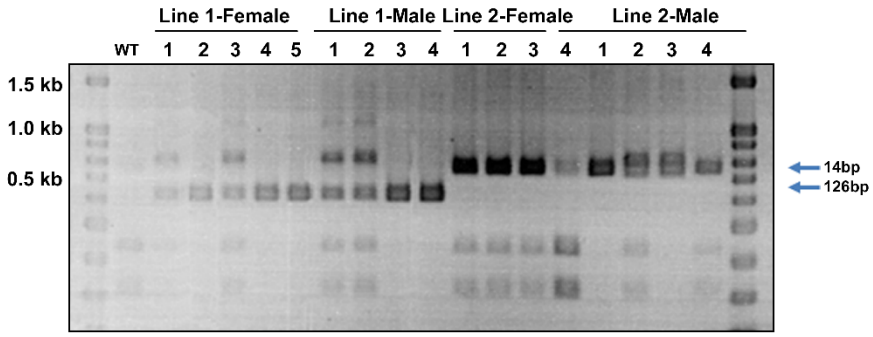
Line 1-Female
Line 1-Male
Line 2-Female
Line 2-Male
WT
1 2 3 4 5
1 2 3 4
1 2 3 4
1 2 3 4
1.5 kb
1.0 kb
0.5 kb
14bp
126bp

Figure II-10. Expression analysis of S5b in the tissues of PSMD5/S5b knockout and WT mice. (**A**) Tissue extracts were collected from 4-week-old wild-type (WT) and S5b knockout (*PSMD5* KO) mice and analyzed by Western blotting. (**B**) Tissue extracts from brain subregion (cortex, hippocampus, striatum, cellebellum) were prepared from 1-month-old wild-type (WT) or S5b knockout (*PSMD5* KO) mice and analyzed by Western blotting.

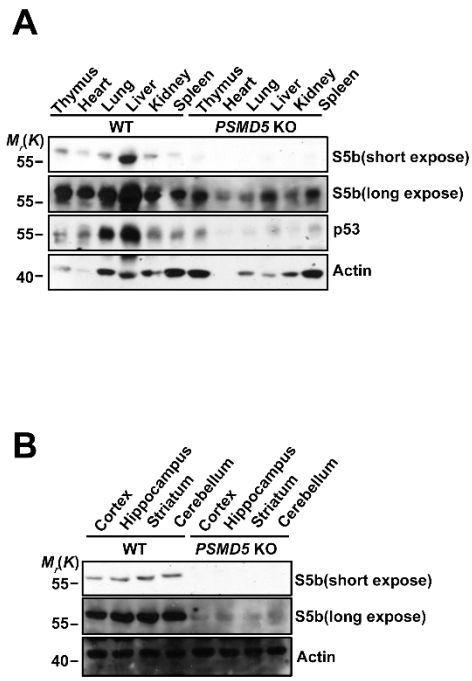
A
Thymus
Heart
Lung
Liver
Kidney
Spleen
Thymus
Heart
Lung
Liver
Kidney
Spleen
WT
PSMD5 KO
M_r(K)
55
55
55
40
S5b(short expose)
S5b(long expose)
p53
Actin
B
Cortex
Hippocampus
Striatum
Cerebellum
Cortex
Hippocampus
Striatum
Cerebellum
WT
PSMD5 KO
M_r(K)
55
55
40
S5b(short expose)
S5b(long expose)
Actin

Figure II-11. Elevated proteasome activity in S5b knockout mice. (A) Tissue extracts were collected from 4-week-old wild-type (WT) and S5b knockout (*PSMD5* KO) mice and measured for proteasome activities using Suc-LLVY-AMC. (**B**) Tissue extracts from brain subregion (cortex, hippocampus, striatum, cerebellum) were prepared from 1-month-old wild-type (WT) or S5b knockout (*PSMD5* KO) mice and analyzed for proteasome activities using Suc-LLVY-AMC.

A

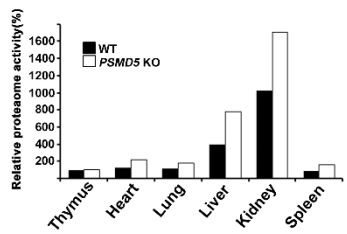
Relative proteaome activity(%)
1600
1400
1200
1000
800
600
400
200
WT
PSMD5 KO
Thymus
Heart
Lung
Liver
Kidney
Spleen

B

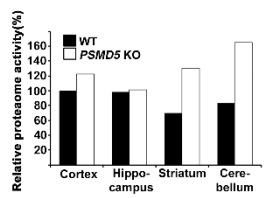
Relative proteaome activity(%)
160
140
120
100
80
60
40
20
WT
PSMD5 KO
Cortex
Hippo-campus
Striatum
Cere-bellum

Figure II-12. Proposed model for the role of GRK2 in S5b-mediated neuronal cell death.

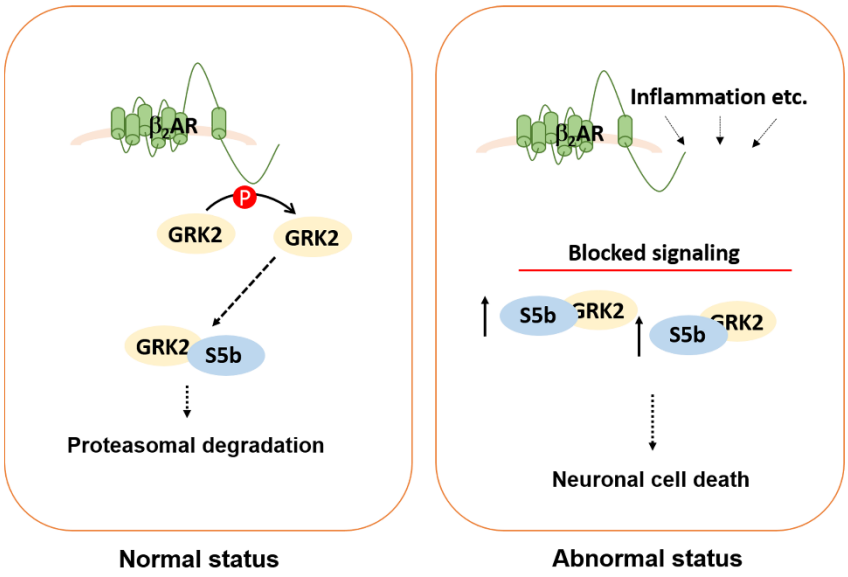

Normal status

Abnormal status

Discussion

Inflammation-induced S5b has a role in early aging and tauopathy (Shim et al., 2012). Like S5b, S5a, a proteasome subunit, is also found in the proteasome complex or as a free form (Shim et al., 2012; Lange et al., 1999; Kiss et al., 2005; Johansson et al., 2008). S5a inhibits intestinal hypersecretion, is a potent anti-inflammatory agent and acts as a neuromodulator (Johansson et al., 2008, 1995; Lönnroth et al., 2003; Davidson and Hickey, 2004; Kim et al., 2005). Because free form of S5a has various roles in addition to a component of proteasome complex (Johansson et al., 2008, 1995; Lönnroth et al., 2003; Davidson and Hickey, 2004; Kim et al., 2005), free form of S5b may have other role irrelevant to the proteasome function, as shown in this manuscript.

S5b Tg mice show early aging phenotype. In addition, I found that the mice did not actively move around in the cage and seemed to be depressed. Thus, I searched putative target of S5b in the mice which might be associated with the phenotype. I found that GRK2 level was significantly down-regulated only in the cortex and hippocampus among brain subregions showing neuronal loss. Since GRK is an essential regulator of GPCR family, I hypothesized that GRK may play a role in such depressed phenotype in S5b

Tg mice. I also raised a possibility that inflammation-induced S5b might affect memory or behavior activity of mice through GRK2 downregulation.

Elevated GRK2 contributes to the pathogenesis of heart failure (Lymperopoulos, 2011; Zhu et al., 2012) and GRK2 is decreased in chronic inflammatory diseases (Vroon et al., 2005). Moreover, inhibition of GRK2 is emerging treatment for heart failure (Cannavo et al., 2013). Consistent to our results, activation of GRK2 protects cell death in neurons (Degos et al., 2013). Low level of GRK2 in sensory neurons is critical for prolongation of hyperalgesia and caused chronic pain (Wang et al., 2011; Ferrari et al., 2012). While GRK2 knockdown in mouse primary cortical neurons sensitizes neurons to excitotoxicity, overexpression of GRK2 is neuroprotective in the models of neurodegeneration (Degos et al., 2013). As mentioned above, GRK2 has tissue- and disease-specific role. Thus, distinct regulation of GRK2 by S5b in the cortex and hippocampus is expectable but remains to be elusive.

Increased S5b induces cell death via caspase activation in neuronal cells and cell death is blocked by the overexpression of GRK2 with kinase activity. As reported, reduced GRK2 influences pain and neuronal cell death (Wang et al., 2011; Ferrari et al., 2012; Degos et al., 2013). While reduced GRK2 is associated with lasting the duration of inflammatory pain (Wang et al., 2011; Ferrari et al., 2012; Eijkelkamp et al., 2010), mechanism of cell death is not clear yet. Nonetheless, a clue that S5b-induced cell death or inflammation

toxicity can be mediated by GRK2 down-regulation may provide a basis for the mode of cell death.

GRK2 is a multidomain protein with various functions and forms very complex interactome (Ribas et al., 2007; Penela et al., 2010; Penela et al. 2009). The expression level and function of GRK2 are tightly regulated and changed in several diseases (Ribas et al., 2007; Penela et al., 2010; Aragay et al., 1998; Rengo et al., 2011). Regulation of GRK2 protein stability by S5b may provide an important clue to understand the molecular pathology. Most of the studies have focused on downstream molecules and kinase cascade of GRK2 (Penela et al., 2003) and little is reported on the regulatory mechanism of GRK2 expression. Our data shows that interaction between S5b and GRK2 reduces both expression level and membrane targeting of GRK2. Because overexpression of S5b reduces the half-life of GRK2 protein and membrane localization of GRK2, it seems that membrane targeting of GRK2 is important for the regulation of GRK2 stability. There is a possibility that S5b suppresses the approach of other kinases to membrane targeting or accelerates interaction with mdm2 to promote its proteasome-dependent degradation (Salcedo et al., 2006; Nogués et al., 2011).

Although brain inflammation just started with many implications in a wide range of diseases, studies have focused on the neurotoxic effects of the cytokine itself through nitric oxide and reactive oxygen species (Block et al., 2007; Vitner et al., 2012). In contrast, this study provide insight into the

contribution of neuroinflammation on the pathology of neurodegenerative diseases through S5b and GRK2. I propose that S5b is a potential regulator linking between inflammation and GRK2-induced neuronal cell death (Figure II-12 A).

References

Deveraux Q, Jensen C & Rechsteiner M (1995) Molecular cloning and expression of a 26 S protease subunit enriched in dileucine repeats. *J Biol Chem* **270**, 23726-23729.

Funakoshi M, Tomko RJ Jr, Kobayashi H & Hochstrasser M (2009) Multiple Assembly Chaperones Govern Biogenesis of the Proteasome Regulatory Particle Base. *Cell* **137**, 887-899.

Park S, Roelofs J, Kim W, Robert J, Schmidt M, Gygi SP & Finley D (2009) Hexameric assembly of the proteasomal ATPases is templated through their C termini. *Nature* **459**, 866-870.

Roelofs J & Finley D (2009) Chaperone-mediated pathway of proteasome regulatory particle assembly. *Nature* **459**, 861-865.

Saeki Y, Toh-E A, Kudo T, Kawamura H & Tanaka K (2009) Multiple proteasome-interacting proteins assist the assembly of the yeast 19S regulatory particle. *Cell* **137**, 900-913.

Gorbea C, Taillandier D & Rechsteiner M (2000) Mapping subunit contacts in the regulatory complex of the 26 S proteasome. S2 and S5b form a tetramer with ATPase subunits S4 and S7. *J Biol Chem* **275**, 875-882.

Barrault MB, Richet N, Godard C, Murciano B, Le Tallec B, Rousseau E, Legrand P, Charbonnier JB, Le Du MH, Guérois R, Ochsenbein F & Peyroche A (2012) Dual functions of the Hsm3 protein in chaperoning and scaffolding regulatory particle subunits during the proteasome assembly. *Proc Natl Acad Sci USA* **109**, E1001-1010.

Shim SM, Lee WJ, Kim Y, Chang JW, Song S & Jung YK (2012) Role of 5b/PSMD5 in proteasome inhibition caused by TNF-α/NFκB in higher eukaryotes. *Cell Rep* **2**, 603-615.

Ribas C, Penela P, Murga C, Salcedo A, García-Hoz C, Jurado-Pueyo M, Aymerich I & Mayor F Jr (2007) The G protein-coupled receptor kinase (GRK) interactome: role of GRKs in GPCR regulation and signaling. *Biochim Biophys Acta* **1768**, 913-922.

Penela P, Murga C, Ribas C, Lafarga V & Mayor F Jr (2010) The

complex G protein-coupled receptor kinase 2 (GRK2) interactome unveils new physiopathological targets. *Br J Pharmacol* **160**, 821-832.

Harris DM, Cohn HI, Pesant S & Eckhart AD (2008) GPCR signalling in hypertension: role of GRKs *Clin Sci (Lond)* **115**, 79-89.

Obrenovich ME, Morales LA & Aliev G (2009) Insights into cerebrovascular complications and Alzheimer disease through the selective loss of GRK2 regulation. *J Cell Mol Med* **13**, 853-865.

Liggett SB (2011) Phosphorylation barcoding as a mechanism of directing GPCR signaling. *Sci Signal* **4**, pe36.

Whalen EJ, Foster MW & Stamler JS (2007) Regulation of beta-adrenergic receptor signaling by S-nitrosylation of G-protein-coupled receptor kinase 2. *Cell* **129**, 511-522.

Vroon A, Kavelaars A & Heijnen CJ (2005) G protein-coupled receptor kinase 2 in multiple sclerosis and experimental autoimmune encephalomyelitis. *J Immunol* **174**, 4400-4406.

Cong M, Perry SJ & Lefkowitz RJ (2001) Regulation of membrane

targeting of the G protein-coupled receptor kinase 2 by protein kinase A and its anchoring protein AKAP79. *J Biol Chem* **276**, 15192-15199.

Cannavo A, Liccardo D & Koch WJ (2013) Targeting cardiac β-adrenergic signaling via GRK2 inhibition for heart failure therapy. *Front Physiol* **4**, 264.

Lange S, Jennische E, Johansson E & Lönnroth I (1999) The Antisecretory Factor—synthesis and intracellular localization in porcine tissues. *Cell Tissue Res* **296**, 607–617.

Kiss P, Szabó A, Hunyadi-Gulyás E, Medzihradszky KF, Lipinszki Z, Pál M & Udvardy A (2005) Zn2+-induced reversible dissociation of subunit Rpn10/p54 of the Drosophila 26 S proteasome. *Biochem J* **391**, 301–310.

Johansson E, Jonson I, Bosaeus M & Jennische E (2008) Identification of flotillin-1 as an interacting protein for antisecretory factor. *Regul Pept* 1**46**, 303-309.

Johansson E, Lönnroth I, Lange S, Jonson I, Jennische E & Lönnroth C (1995) Molecular cloning and expression of a pituitary gland protein modulating intestinal fluid secretion. *J Biol Chem* **270**, 20615–20620.

Lönnroth I, Lange S, Jennische E, Johansson E, Jonson I & Torres J (2003) Cholera toxin protects against action by Clostridium difficile toxin A. The role of atisecretory factor in intestinal secretion and inflammation in rat. *APMIS* **111**, 969–977.

Davidson TS & Hickey WF (2004) Antisecretory factor is regulated by inflammatory mediators and influences the severity of experimental autoimmune encephamyelitis *J Leukoc Biol* **76**, 835–844.

Kim M, Wasling P, Xiao MY, Jennische E, Lange S & Hanse E (2005) Antisecretory factor modulates GABAergic transmission in the rat hippocampus. *Regul Pept* **129**, 109–118.

Lymperopoulos A (2011) GRK2 and β-arrestins in cardiovascular disease: Something old, something new. Am J Cardiovasc Dis 1, 126–137.

Zhu W, Petrashevskaya N & Xiao RP (2012) Gi-biased β2AR signaling links GRK2 upregulation to heart failure. *Circ Res* **110**, 265-274.

Wang H, Heijnen CJ, Eijkelkamp N, Garza Carbajal A, Schedlowski M, Kelley KW, Dantzer R & Kavelaars A (2011) GRK2 in sensory neurons regulates epinephrine-induced signalling and duration of mechanical hyperalgesia. *Pain* **152**, 1649-1658.

Ferrari LF, Bogen O, Alessandri-Haber N, Levine E, Gear RW & Levine JD (2012) Transient decrease in nociceptor GRK2 expression produces long-term enhancement in inflammatory pain. *Neuroscience* **222**, 392-403.

Degos V, Peineau S & Gressens P (2013) G protein-coupled receptor kinase 2 and group I metabotropic glutamate receptors mediate inflammation-induced sensitization to excitotoxic neurodegeneration. *Ann Neurol* **73**, 667-678.

Eijkelkamp N, Heijnen CJ & Kavelaars A (2010) GRK2: a novel cell-specific regulator of severity and duration of inflammatory pain. *J Neurosci* **30**, 2138-2149.

Penela P, Ribas C, Aymerich I & Mayor F Jr (2009) New roles of G protein-coupled receptor kinase 2 (GRK2) in cell migration. *Cell Adh Migr* **3**, 19-23.

Aragay AM, Ruiz-Gómez A, Penela P, Sarnago S, Elorza A, Jiménez-Sainz MC & Mayor F Jr (1998) G protein-coupled receptor kinase 2 (GRK2): mechanisms of regulation and physiological functions. *FEBS Lett* **430**, 37-40.

Rengo G, Lymperopoulos A, Leosco D & Koch WJ (2011) GRK2 as a novel gene therapy target in heart failure. *J Mol Cell Cardiol* **50**, 785-792.

Penela P, Ribas C & Mayor F Jr (2003) Mechanisms of regulation of the expression and function of G protein-coupled receptor kinases. *Cell Signal* **15**, 973-981.

Salcedo A, Mayor F Jr & Penela P (2006) Mdm2 is involved in the ubiquitination and degradation of G-protein-coupled receptor kinase 2. *EMBO J* **25**, 4752-4762.

Nogués L, Salcedo A, Mayor F Jr & Penela P (2011) Multiple scaffolding functions of {beta}-arrestins in the degradation of G protein-coupled receptor kinase 2. *J Biol Chem* **286**, 1165-1173.

Block ML, Zecca L & Hong JS (2007) Microglia-mediated neurotoxicity: uncovering the molecular mechanisms. *Nat Rev Neurosci* **8**, 57-69.

Vitner EB, Farfel-Becker T, Eilam R, Biton I & Futerman AH (2012) Contribution of brain inflammation to neuronal cell death in neuronopathic forms of Gaucher's disease. *Brain* **135**, 1724-1735.

Kim JY, Kim DH & Chang JW (2012) Soluble intracellular adhesion molecule-1 secreted by human umbilical cord blood-derived mesenchymal stem cell reduces amyloid-β plaques. *Cell Death Differ* **19**, 680-691.

국문 초록

프로테아좀은 유비퀴틴-프로테아좀 체계(UPS)에서 다양한 단백질을 분해하는 거대한 단백질 복합체이다. 항상성을 유지하기 위해 역할을 하는 수많은 기질들이 이 정교한 과정에 의해 분해된다. 또한, 이 UPS의 비정상적인 조절이나 복합체의 이상은, 암이나 면역체계 혹은 퇴행성 신경 질환에 연관되어 있다. 하지만 이 정교한 체계가 세포 내 수많은 신호전달 체계에서 어떻게 조절되는 지에 대해서는 잘 알려져 있지 않다. 따라서 새로운 프로테아좀 조절인자를 발견하는 것은, 프로테아좀 기능이상과 관련된 여러 질병들의 발병 혹은 UPS-관련 세포 내 기능을 이해하는 데 중요하다. 프로테아좀 활성도를 조절하는 새로운 프로테아좀 조절자를 밝히기 위해, Degron-GFP 와 cDNA 유전자 모음을 이용해 세포 기반 기능성 동정 시스템을 구축하였다. 이 연구에서, Degron-GFP 와 cDNA 유전자에 기반한 기능성 동정 시스템을 통해 iRhom1 을 프로테아좀 기능 활성자로 찾아내었다. iRhom1 의 발현 정도는 프로테아좀 복합체의 활성과 조립을 조절하였다. iRhom1 은 소포체 자극제에 의해 그 발현양이 조절되며, 그 증가는 특히 소포체 관련-

마이크로좀에서의 프로테아좀 활성과 조립을 증가시켰다. iRhom1 은 20S 프로테아좀 조립 샤페론 PAC1 과 PAC2 와 결합하고, 이합체화를 통해 단백질들의 안정성에 영향을 주었다. 또한 iRhom 이 결핍된 초파리는 돌연변이 헌팅턴 초파리의 거친 눈 현상을 더욱 더 악화시켰고, 인간 iRhom1 과 초파리 iRhom 을 과발현 시킬 경우 그러한 증상이 완화되는 것으로 확인되었다..

S5b 는 이전 연구를 통해 효모 프로테아좀 조립 샤페론과 포유류 26S 프로테아좀의 음성 조절자로 밝혀졌다. GRK2 는 신경세포에서 세포 사멸 매개자로 생각되고 있으나, GRK2 발현 조절에 대해서는 잘 알려져있지 않다. 이 연구에서 나는 S5b 를 통한 GRK2 을 조절을 신경세포와 쥐 모델에서 밝히고자 한다. GRK2 는, 만성 염증 모델인 S5b 형질전환 쥐의 뇌 피질과 해마 부위에서 감소하는 것으로 밝혀졌고, 쥐 해마 세포 HT22 에서 S5b 의 과발현 또한 GRK2 의 양을 감소시켰다. S5b 의 감소는 GRK2 양을 증가시켰는데, 이는 S5b 의 프로테아좀 기능 활성저하와는 관계없이, GRK2 단백질의 안정성 유지를 통해서이다. GRK2 와 인산화 불활성 돌연변이 GRK2 K220R 는 쥐의 뇌 피질과 HT22 세포에 S5b 의 카르복실 말단 부위를

통해 결합하는 것하며, 이 카르복실 말단 부위 역시 GRK2 의 양을 감소시켰다. 세포질 염색, 분획법, 표면 바이오틸 실험 등을 통한 여러 방법에서, GRK2 의 막으로의 이동이 S5b 의 발현에 영향을 받는 것으로 밝혀졌다. 또한 S5b 에 의한 신경 독성이, 인산화 불활성 돌연변이 GRK2 K220R 이 아닌 정성 GRK2 의 발현으로 인해 줄어드는 것을 확인하였다. 따라서, S5b 는 신경세포에서, 신경 독성 매개자인 GRK2 를 조절하여 그 독성을 보이는 것으로 생각되며, 신경 세포 사멸에서 GRK2 의 새로운 조절자라는 또 다른 역할을 보여주고 있다. 또한 *Psmd5*/S5b 유전자 제거 생쥐가 Cas9/CRISPR 방법을 통해 생산되었고, 연령에 따른 프로테아좀 활성을 보이고 있다. 종합하여, S5b 는 질병 상황에서 프로테아좀 활성을 조절함과 동시에, GRK2 를 통해 신경세포 사멸에 관여하는 다양한 역할을 하고 있다. 결론적으로, 나는, 스트레스 상황에서 프로테아좀을 조절하는 새로운 신호전달 체계와 S5b 의 프로테아좀 활성 기능과 무관한, 신경세포의 사멸에 관련된 새로운 역할에 대해 제시하고자 한다.